A Computational Iteration Method to Analyze Mechanics of Timing Belt Systems with Non-Circular Pulleys

Li Tan

Thesis submitted to the Faculty of the

Virginia Polytechnic Institute and State University

in partial fulfillment of the requirements for the degree of

Master of Science

in

Mechanical Engineering

Robert G. Parker, Chair

Lei Zuo

Corina Sandu

August 10, 2018

Blacksburg, Virginia

Keywords: Timing Belt, Non-circular Pulley, Torque.

A Computational Iteration Method to Analyze Mechanics of Timing Belt Systems with Non-Circular Pulleys

Li Tan

(ABSTRACT)

A quasi-static computational model is developed to calculate the belt load distributions and the torques around pulleys for different timing belt systems. The simplest system is a two-pulley system with one oval pulley and one circular pulley. This computational model is then extended to a two-pulley system with one special-shaped pulley and finally generalized to determine the load conditions for a multi-pulley system with multiple special-shaped pulleys. Belt tooth deflections, tooth loads, belt tension distributions, friction forces, and the effect of friction hysteresis have been taken into consideration. Results of these quantities are solved by a nested numerical iteration method. Periodic torques generated by the varied radius of noncircular pulley are calculated by this computational model to cancel the undesired external cyclic torque, which will increase the life of timing belts.

A Computational Iteration Method to Analyze Mechanics of Timing Belt Systems with Non-Circular Pulleys

Li Tan

(GENERAL AUDIENCE ABSTRACT)

Timing belt systems, usually consisting of a toothed belt and multiple pulleys, are used in many mechanical devices, especially in the internal combustion engine to synchronize the rotation of the crankshafts and the camshafts. When the system operates, the belt teeth will be transmitted by the pulley teeth meshed with them. Timing belt drives can make sure that the engines valves open and close properly due to their precise transmission ratio. In this thesis, a quasi-static computational model is developed to calculate the belt load distributions and the torques around pulleys for different timing belt systems. The simplest system is a two-pulley system with one oval pulley and one circular pulley. This computational model is then extended to a two-pulley system with one special-shaped pulley and finally generalized to determine the load conditions for a multi-pulley system with multiple special-shaped pulleys. Belt tooth deflections, tooth loads, belt tension distributions, friction forces, and the effect of friction hysteresis have been taken into consideration. Results of these quantities are solved by a nested numerical iteration method. Periodic torques generated by the varied radius of noncircular pulley are calculated by this computational model to cancel the undesired external cyclic torque, which will increase the life of timing belts.

Contents

List of Figures

List of Tables

Chapter 1

Introduction

Timing belt drives have been widely used in mechanical devices, especially in internal combustion engines to synchronize the rotation of the crankshaft and the camshafts. Timing belts are characterized by the teeth on their inside surface, which greatly improves the accuracy of transmission ratio by meshing with the corresponding pulley teeth.

Considerable research has been done on the load distributions of timing belt systems due to their wide applications, and the models of timing-belt system with circular pulleys for quasi-static loading have existed since 1978. Gerbert et al. [1] first developed a spring-based model to analyze load distributions in timing belts and preliminarily considered the effect of friction. Further steps in the study of loading conditions were achieved by analyzing belt properties, pretensions, and the pitch difference between the belt and the pulley [2][3]. Shimizu and Fujii [4] and Karolev and Gold [5] presented models transmitting variable torques respectively and the latter put forward the idea of friction hysteresis. Childs et al. [6] discussed tooth distortions generated in partial meshing and the resulting tooth force variations. Johannesson and Distner [7] proposed a multi-body model for modern belt profiles with the consideration of friction history. With the use of timing belt drive system, a periodic fluctuating torque caused by the opening and closing of the intake and exhaust valves is found in the internal combustion engine. A resonance occurs when the frequency of this

fluctuating torque is close to the natural frequency of the timing belt systems. Therefore, this fluctuating torque can lead to the speed fluctuation and the angular displacement fluctuation (also known as torsional vibration) in the timing belt systems. The best cure for this problem is to attack the cause right at the source by introducing a corrective torque acting on the camshaft. In this situation, the fluctuating torque caused by the valve train can be reduced or substantially cancelled. One way that is widely adopted is to replace the circular pulley with an oval pulley at the crankshaft. The rotation of the oval pulley results in the fluctuations of span length that can generate a corrective torque at the camshaft [8]. Only little researches have been done in this field. Zhu et al. [9][10] established a dynamic model to search for an optimal design of the oval pulley to minimize torsional vibrations of the system. However, in their study, only pitch profile of the timing belt drive system was considered. It is reasonable to develop a spring-based model suitable for timing belt systems with an oval pulley to figure out the influences of the oval pulley and the meshing between belt teeth and pulley teeth on the load distributions in timing belts.

Iteration methods have already been used in many researches to study the mechanics of drive system. Kong and Parker [11] used an iteration method to deal with initially unknown belt-pulley contact points resulted from the inclusion of belt bending stiffness. Kagotani and Ueda [12] used a similar idea of iteration to calculate belt tensions in synchronous belt drive with eccentric pulleys.

In this work, a computational model for a timing belt system with noncircular pulleys is built by combining the iteration method with the previous spring-based models. The periodic torque generated by the rotation of the noncircular pulley is then calculated. The key step of using iteration method is to find the compatibility conditions for the timing belt systems, which is necessary to calculate the belt tension distributions.

Section 2.1 presents a general spring-based model for timing belt systems. Section 2.2 describes how to combine a spring-based model with iteration method to handle the unknown free-span tensions brought by one oval pulley. Section 2.3 presents the extension of the com-

putational model for more complex timing-belt systems. Two systems are considered. One is the two-pulley system with an inflated rounded square pulley and the other one is the three-pulley system with two oval pulleys. Section 2.4 shows the numerical results for these three systems and several conclusions are summarized in Chapter 3.

Chapter 2

Analysis of load distributions

The analysis mainly focuses on two-pulley timing belt system with an oval pulley. A belt in contact with two pulleys is shown in Figure 2.1. Previous researches mostly investigate the influence of external transmitted load on tension distributions in the timing belt systems with circular pulleys. In their cases, tensions in free spans are known and used to calculate the tension distributions along the belt. In this work, one circular pulley is replaced by an oval pulley and external torques acted on pulleys are assumed to be zero. The tensions in free spans become unknown and the varied radius of the oval pulley is the only reason for the force change in timing belts when the system operates. In this situation, configurations of pulleys should be specified to determine the tension distributions in the timing belt.

2.1 System model

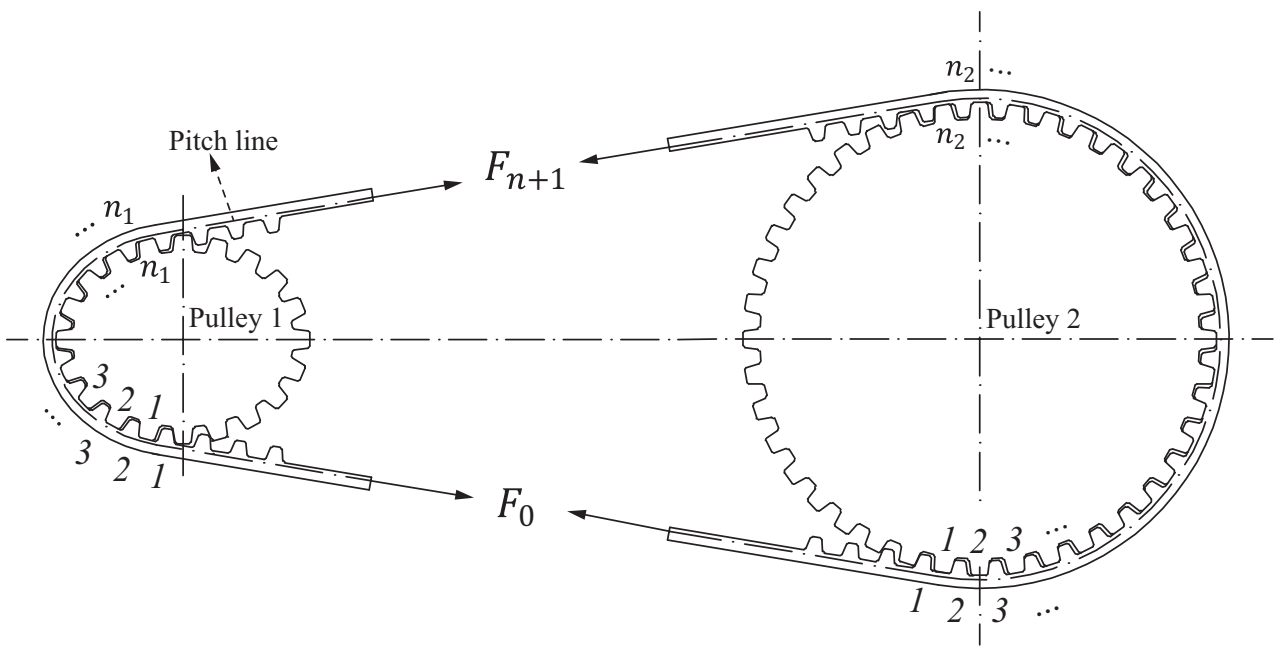

Figure 2.1: Indexes of pulley teeth and belt teeth

As the oval pulley rotates in one direction, the variation of its radius will change the stretched lengths of timing belts. The free-span tensions and the torque directions will change accordingly. For the convenience of description, as shown in Figure 2.1, the positions of pulley teeth and belt teeth are numbered from the first tooth engagement to the last tooth engagement. Meanwhile, the oval pulley and the circular pulley are regarded as pulley 1 and pulley 2 respectively. The pitch line is identical to the neutral bending axis of the belt.

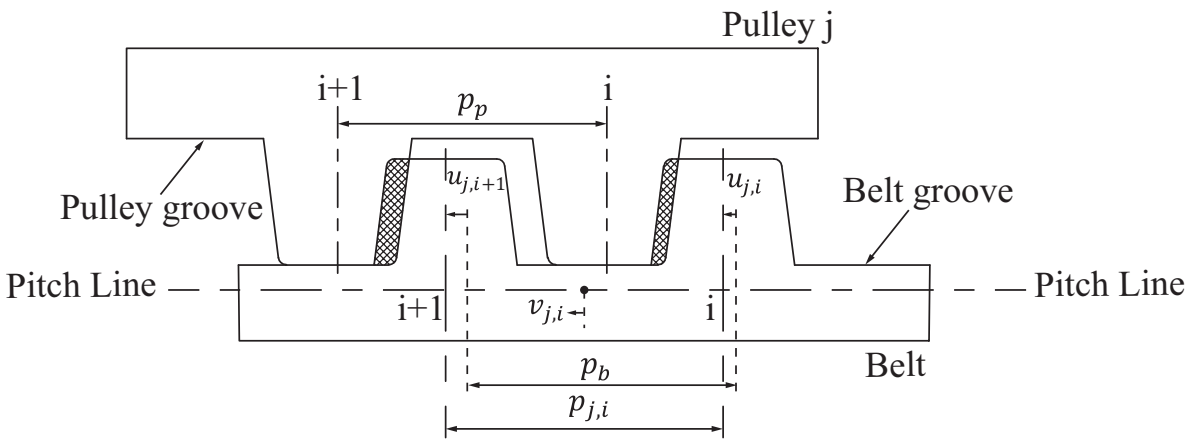

Figure 2.2: Deflections of belt teeth, and meshing between belt and pulley. The dashed lines denote the unstretched positions of the belt teeth centerlines and the mid points of the belt pitch between two adjacent belt teeth. The long dashed short dashed lines denote the pulley teeth centerlines and the stretched positions of the belt teeth centerlines

Figure 2.2 is the sketch of the meshing between belt and pulley in tangential direction for one belt pitch. p_p is the pulley pitch and this length will not change with force. $p_{j,i}$ is the stretched length of the belt pitch between two adjacent belt teeth and p_b is the unstretched length of the belt pitch between two adjacent belt teeth. The difference between the pulley pitch and the unstretched belt pitch is called the pitch difference. i is the index of the pulley tooth and belt tooth. $j(j = 1, 2)$ denotes the pulley. From Figure 2.2, the difference between the stretched belt pitch and the unstretched belt pitch is

$$p_{j,i} - p_b = u_{j,i+1} - u_{j,i} \tag{2.1.1}$$

where $u_{j,i}$ and $u_{j,i+1}$ are the elastic deflections of the belt teeth i and $i + 1$. The elastic deflection of the belt groove $v_{j,i}$ is assumed to be the same as the elastic deflection of the unstretched belt pitch mid-point. Shaded areas represent loads acting between the tooth flanks of belt teeth and pulley teeth. These tooth contact loads are referred to as tooth load. When the belt tooth i just touches the pulley tooth i (tooth load between belt tooth and pulley tooth i is zero), the distance between the centerlines of the belt tooth i and the

pulley tooth i is d_w. Backlash b is the clearance between belt tooth and pulley groove. The relationship between the d_w and b is

$$d_w = \frac{p_p - b}{2} \tag{2.1.2}$$

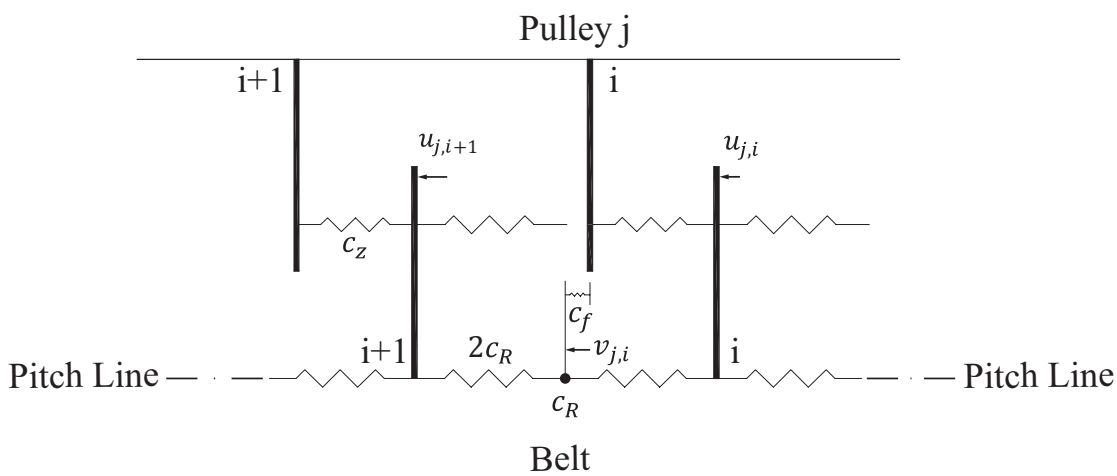

Figure 2.3: Meshing model. The thick solid lines, coinciding with the teeth centerlines, denote the positions of belt teeth and pulley teeth.

Figure 2.3 is the meshing model for the timing belt drive. Similar model is first developed by Karolev and Gold[5]. The thick solid lines denote the belt teeth and pulley teeth. These solid lines coincide with the centerlines of the corresponding teeth. Downward lines represent the pulley teeth and upward lines represent the belt teeth. In this meshing model, belt teeth and belt grooves are modeled as elastic stiffnesses with stiffness constants c_z and c_f respectively. Due to the influence of the friction force (introduced later), one belt pitch between two adjacent belt teeth is modeled as two stiffnesses in series. Each stiffness has a stiffness constant $2c_R$ and the total stiffness of one belt pitch is c_R.

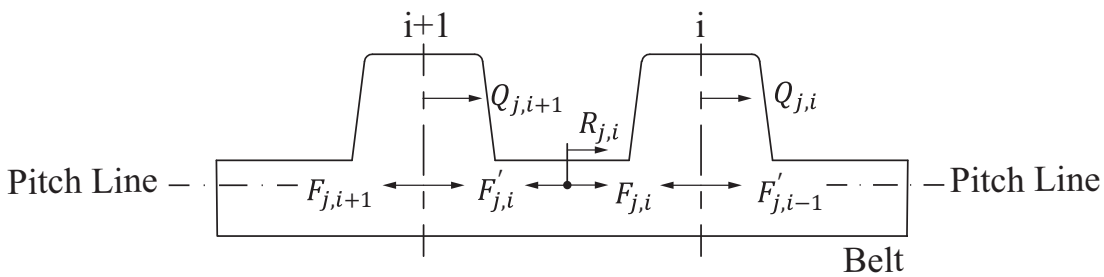

Figure 2.4: Free body diagram of belt teeth and one belt pitch between two adjacent belt teeth. The thick solid lines, coinciding with the teeth centerlines, denote the positions of belt teeth.

Figure 2.4 is the free body diagram of one belt pitch between belt teeth i and $i+1$. In this work, the mass of the belt, the pitch difference between the belt and the pulley, and the inclination of the belt tooth are neglected. Static force balances can then be established. For belt tooth i, the force balance in tangential direction requires that

$$Q_{j,i} = F_{j,i} - F'_{j,i-1} \tag{2.1.3}$$

Depending on the relation between the deflection $u_{j,i}$ of the belt tooth i and the backlash b, tooth load $Q_{j,i}$ can also be calculated by the elongation of the stiffness c_z in three different cases like below

$$u_{j,i} > 0 \Longrightarrow Q_{j,i} = u_{j,i} c_z \quad (Q_{j,i} > 0) \tag{2.1.4a}$$

$$0 \geq u_{j,i} \geq -b \Longrightarrow \; Q_{j,i} = 0 \tag{2.1.4b}$$

$$-b > u_{j,i} \Longrightarrow \; Q_{j,i} = (u_{j,i} + b)\, c_z \quad (Q_{j,i} < 0) \tag{2.1.4c}$$

For trapezoidal shape timing belts, belt grooves contact with the top lands of the pulley teeth, while the pulley grooves have no contact with the top lands of the belt teeth. Therefore, friction force is assumed to only exist between the belt grooves and the top lands of pulley

teeth. In the belt pitch between belt tooth i and belt tooth $i+1$, friction force $R_{j,i}$ is

$$R_{j,i} = F'_{j,i} - F_{j,i} \tag{2.1.5}$$

Following [5], this friction force is proportional to the elastic deflection $v_{j,i}$ of the belt groove and can be calculated by

$$R_{j,i} = v_{j,i} c_f \tag{2.1.6}$$

The elongation of one belt pitch between belt tooth i and belt tooth $i+1$ is the sum of the elongations of the two corresponding half belt pitches

$$p_{j,i} - p_b = \frac{F_{j,i} + F'_{j,i}}{2c_R} \tag{2.1.7}$$

where $p_{j,i}$ and p_b are the stretched length and the unstretched length of one belt pitch respectively. $F_{j,i}/2c_R$ is the elongation of the half belt pitch between the tooth i and the belt pitch mid-point, and $F'_{j,i}/2c_R$ is the elongation of the half belt pitch between the belt pitch mid-point and the tooth $i+1$. From Equations 2.1.7 and 2.1.1, solution for $u_{j,i+1}$ is

$$u_{j,i+1} = u_{j,i} + \frac{F_{j,i} + F'_{j,i}}{2c_R} \tag{2.1.8}$$

The operation of the timing belt system is pursued step by step. The friction force in current step is affected by the friction force in the preceding step and this phenomenon is called friction hysteresis [5].

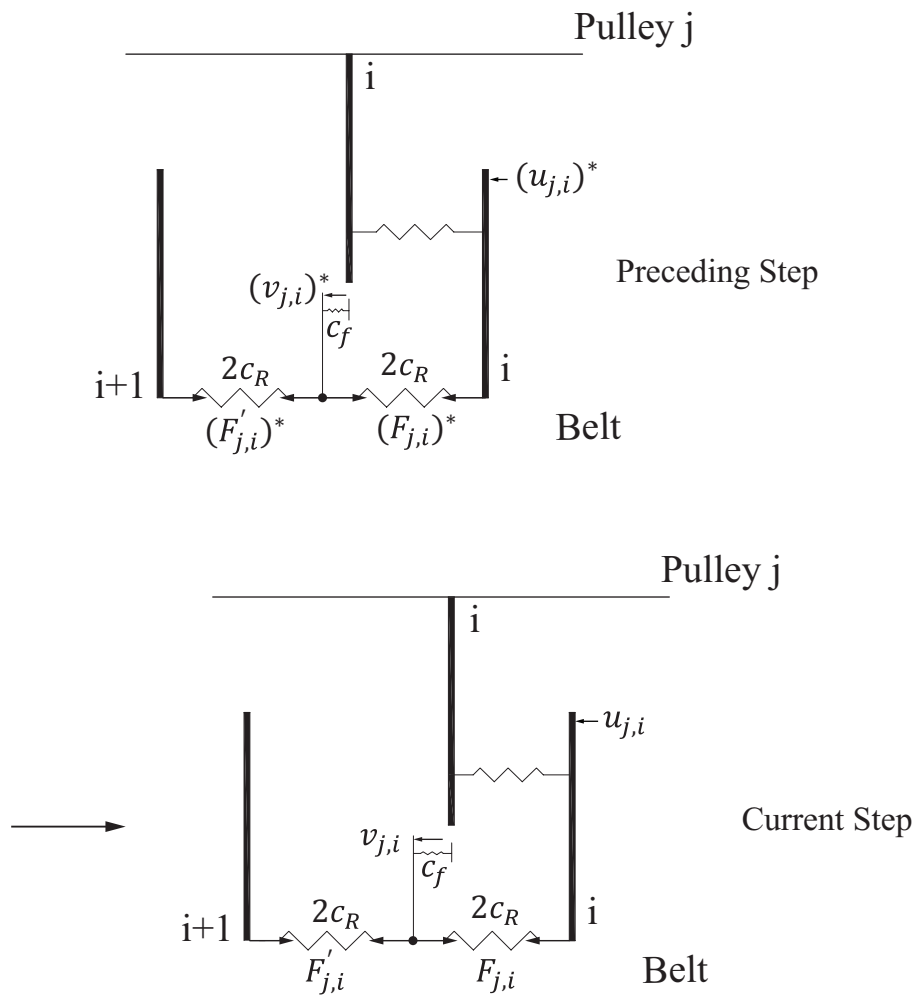

Figure 2.5: Relative displacements between the preceding and the current rotation steps

Consider the case when the pulley tooth i takes a step to the right (as shown in Figure 2.5,). To find the relation between the friction forces in the preceding step and the current step, the elongation of half belt pitch between the belt pitch mid-point and the belt tooth i is calculated. For the preceding step,

$$(v_{j,i})^* - (u_{j,i})^* = \frac{(F_{j,i})^*}{2c_R} \tag{2.1.9}$$

where $()^*$ denotes the values in the preceding step. For the current step,

$$v_{j,i} - u_{j,i} = \frac{F_{j,i}}{2c_R} \tag{2.1.10}$$

Subtraction of Equation 2.1.9 from Equation 2.1.10 leads to the relative deflection $\Delta v_{j,i}$ of belt pitch mid-point

$$\begin{aligned} \Delta v_{j,i} &= v_{j,i} - (v_{j,i})^* \\ &= u_{j,i} - (u_{j,i})^* + \frac{F_{j,i}}{2c_R} - \frac{(F_{j,i})^*}{2c_R} \end{aligned} \tag{2.1.11}$$

From Equation 2.1.11, the friction force in the current step can be expressed by

$$v_{j,i} = u_{j,i} - (u_{j,i})^* + \frac{F_{j,i} - (F_{j,i})^*}{2c_R} + (v_{j,i})^* \tag{2.1.12}$$

2.2 Analysis of timing belt system using iteration method

As introduced before, tensions in free spans are unknown in this work. For a two-pulley system, there are two free-span tensions. If these two tensions can be found, all other values can be determined accordingly. A one-to-one relationship between the belt tensions and the length changes of the corresponding belt pitches can be established. Therefore, it is reasonable to investigate the elongation of belt pitch line, which will reflect the tensions in the belt. To determine the two free-span tensions, two compatibility conditions for the two different parts of the belt pitch line are needed in iteration procedure. Detailed process will be presented below.

2.2.1 Compatibility conditions

The schematic diagram of stretched pitch profile is shown in Figure 2.6. Total pitch line is divided into four parts: AB, BC, CD, and AD. Lengths of these four parts are denoted by l_{AB}, l_{BC}, l_{CD}, and l_{AD}. A, B, C, D are tangent points, and lines AB and CD are common

tangent lines to the pitch oval and the pitch circle. O_1 and O_2 are the centers of the oval pulley and the circular pulley. θ_A and θ_D are the counterclockwise angles between O_1A and O_1D and the semi-major axis of the oval pulley. θ_B and θ_C are the clockwise angles between O_2B and O_2C and O_2H. These four angles will change as pulleys rotate.

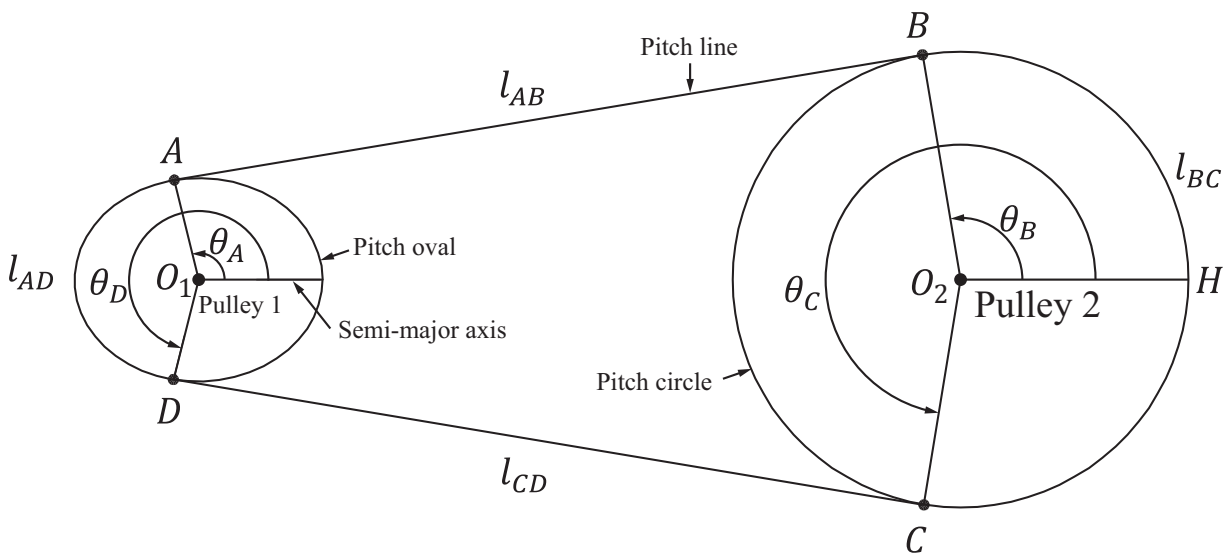

Figure 2.6: Pitch profile of the two-pulley system with an oval pulley. O_2H is parallel to the horizontal line.

Due to the existence of the oval pulley, the method to calculate the arc length of an oval will be presented. With respect to the very small eccentricity of the oval pulley, the radius $R(\varphi)$ depending on φ is approximately expressed by

$$R(\varphi) = R_1 + (\varepsilon/2)\, cos2\varphi \tag{2.2.1}$$

where the angle φ is measured relative to the semi-major axis, R_1 is the radius of an equivalent circular pulley (the equivalent circular pulley has the same circumference as the oval pulley), and ε is the difference in diameter between the oval and the equivalent circular pulley, as indicated on Figure 2.7. The arclength ds of the oval pulley between arbitrary angle φ and $\varphi + d\varphi$ depends on the values of the radius at the angle φ and $\varphi + d\varphi$ marked on Figure 2.7 as $R(\varphi)$ and $R(\varphi) + \frac{dR}{d\varphi}d\varphi$

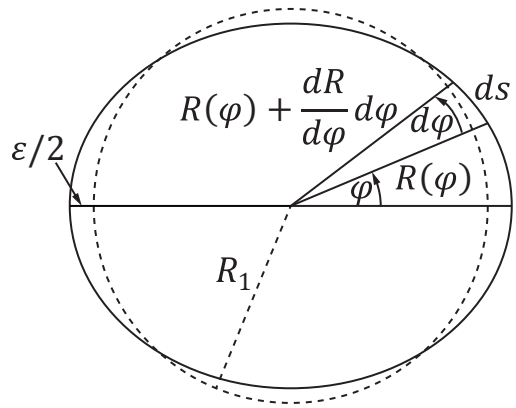

Figure 2.7: Sketch showing how to calculate the length of an arc for a non-circular pulley

According to the "law of cosines", the following relationship between ds and $d\varphi$ is found

$$ds^2 = [R(\varphi)]^2 + \left[R(\varphi) + \frac{dR}{d\varphi}d\varphi\right]^2 - 2R(\varphi)\left[R(\varphi) + \frac{dR}{d\varphi}d\varphi\right] cos(d\varphi) \tag{2.2.2}$$

When φ is very small, Equation 2.2.2 simplifies to

$$ds = \sqrt{[R(\varphi)]^2 + \left(\frac{dR}{d\varphi}\right)^2} d\varphi \tag{2.2.3}$$

Therefore, the arclength of the oval pulley between two arbitrary angles φ_1 and φ_2 is

$$s = \int_{\varphi_2}^{\varphi_1} \sqrt{[R_1 + (\varepsilon/2)\, cos2\varphi]^2 + (-\varepsilon sin2\varphi)^2} d\varphi \tag{2.2.4}$$

For practical timing belt drive, ε is much less than R_1. In this case, the second term in Equation 2.2.4 is neglected to get

$$\begin{aligned} s &= \int_{\varphi_2}^{\varphi_1} [R_1 + (\varepsilon/2)\, cos2\varphi]\, d\theta \\ &= R_1(\varphi_2 - \varphi_1) + (\varepsilon/4)(sin2\varphi_2 - sin2\varphi_1) \end{aligned} \tag{2.2.5}$$

To find the compatibility conditions, free spans are first investigated. The boundaries of the free spans have close relations with the boundaries of meshed area. Therefore, it is important

to figure out the relations between the belt teeth and pulley teeth in these boundary regions.

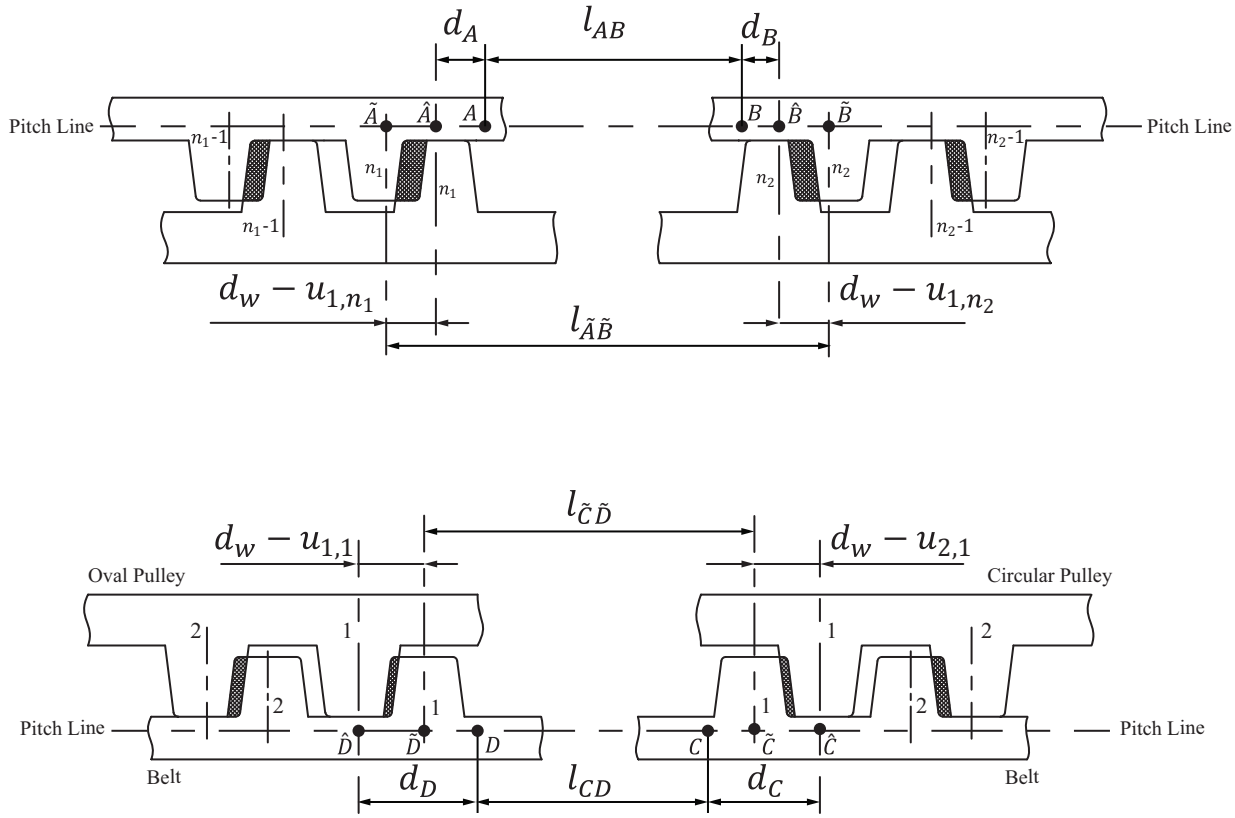

Figure 2.8: Relations between pulley teeth and belt teeth at the boundary region of free span

In Figure 2.8, $\widetilde{A}$, $\widetilde{B}$, $\widetilde{C}$, $\widetilde{D}$ are the intersection points between the pitch line and the centerlines of the meshed belt teeth nearest to tangent points A, B, C, D; $\hat{A}$, $\hat{B}$, $\hat{C}$, $\hat{D}$ are the intersection points between the pitch line and the centerlines of the meshed pulley teeth nearest to tangent points. As indicated in Figure 2.8, stretched lengths of the spans $\widetilde{A}\widetilde{B}$ and $\widetilde{C}\widetilde{D}$ can be calculated geometrically as

$$l_{\widetilde{A}\widetilde{B}} = l_{AB} + d_A + d_B + 2d_w - u_{1,n_1} - u_{2,n_2} \tag{2.2.6}$$

$$l_{\widetilde{C}\widetilde{D}} = l_{CD} + d_C + d_D - 2d_w + u_{1,1} + u_{2,1} \tag{2.2.7}$$

In Equation 2.2.6 and Equation 2.2.7, $u_{1,1}$ and u_{1,n_1} are the deflections of the belt tooth 1

and n_1 meshed with the oval pulley. $u_{2,1}$ and u_{1,n_2} are the deflections of the belt tooth 1 and n_2 meshed with the circular pulley. d_w is the unstretched length between the centerlines of two mating teeth. d_A, d_B, d_C, d_D represent the distances between tangent points A, B, C, D and intersection points $\hat{A}$, $\hat{B}$, $\hat{C}$, $\hat{D}$. The stretched length l_{AB} of free span AB can be computed from the coordinates of tangent points A and B as

$$l_{AB} = \sqrt{(x_A - x_B)^2 + (y_A - y_B)^2} \tag{2.2.8}$$

The stretched length of span CD can be calculated similarly as

$$l_{CD} = \sqrt{(x_C - x_D)^2 + (y_C - y_D)^2} \tag{2.2.9}$$

(x_A, y_A), (x_B, y_B), (x_C, y_C), (x_D, y_D) are the coordinates of tangent points A, B, C, D respectively. Numerical solutions of (x_A, y_A) and (x_B, y_B) can be got from equations below

$$f_1(x_A, y_A) = \frac{(x_A - x_1)^2}{(a_1)^2} - \frac{(y_A - y_1)^2}{(a_2)^2} - 1 = 0 \tag{2.2.10a}$$

$$f_2(x_B, y_B) = (x_B - x_2)^2 - (y_B - y_2)^2 - (R_2)^2 = 0 \tag{2.2.10b}$$

$$R_2 = \frac{|kx_2 - y_2 + y_B - kx_B|}{\sqrt{k^2 + 1}} \tag{2.2.10c}$$

$$k = -\frac{\frac{\partial f_1}{\partial x_A}(x_A, y_A)}{\frac{\partial f_1}{\partial y_A}(x_A, y_A)} \tag{2.2.10d}$$

$$-\frac{\frac{\partial f_1}{\partial x_A}(x_A, y_A)}{\frac{\partial f_1}{\partial y_A}(x_A, y_A)} = \frac{y_A - y_B}{x_A - x_B} \tag{2.2.10e}$$

In Equation 2.2.10, f_1 and f_2 are the expressions for the oval pulley and the circular pulley in the orthogonal coordinate system. If the equations for the pulleys are expressed in the other coordinate system, they should be transformed into the orthogonal coordinate system. If only important points on the pulleys are specified, the approximate equations in the orthogonal coordinate system should be set up. (x_1, y_1) and (x_2, y_2) are the center coordinates of the oval pulley and the circular pulley. a_1 and a_2 represent the lengths of

the semi-major and semi-minor axes of the oval pulley respectively. R_2 is the radius of the circular pulley. Equation 2.2.10c is the formula to calculate the distance from a point (the center of the circular pulley O_2) to a line (AB). k is the slope of the line AB. Equation 2.2.10e displays the two expressions for the slope of the line AB. (x_C, y_C) and (x_D, y_D) can be solved similarly.

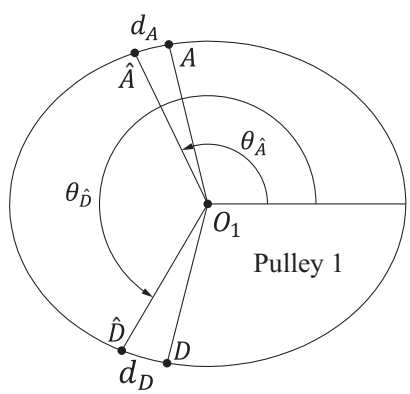

Figure 2.9: Sketch showing how to calculate d_A and d_D

With the help of the arclength formula, d_A and d_D, as indicated on Figure 2.9, can be determined by

$$d_A = R_1\left(\theta_{\hat{A}} - \theta_A\right) + (\varepsilon/4)(sin2\theta_{\hat{A}} - sin2\theta_A) \tag{2.2.11}$$

$$d_D = R_1\left(\theta_D - \theta_{\hat{D}}\right) + (\varepsilon/4)(sin2\theta_D - sin2\theta_{\hat{D}}) \tag{2.2.12}$$

where $\theta_{\hat{A}}$ and $\theta_{\hat{D}}$ are the angles between $O_1\hat{A}$ and $O_1\hat{D}$ and the semi-major axis of the oval pulley. These two angles will change with the rotation of the oval pulley. θ_A and θ_D are the angles between O_1A and O_1D and the semi-major axis of the oval pulley as introduced before.

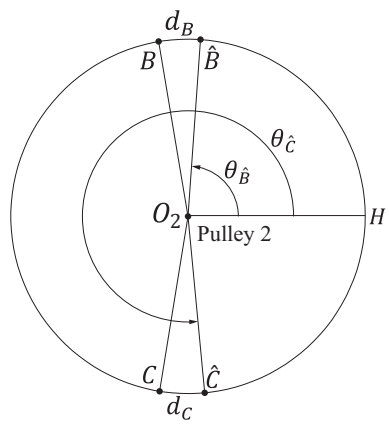

Figure 2.10: Sketch showing how to calculate d_B and d_C. O_2H is parallel to the horizontal line.

d_B and d_C, as indicated on Figure 2.10, can be determined by

$$d_B = R_2 \left(\theta_B - \theta_{\hat{B}}\right) \tag{2.2.13}$$

$$d_C = R_2 \left(\theta_{\hat{C}} - \theta_C\right) \tag{2.2.14}$$

where $\theta_{\hat{B}}$ and $\theta_{\hat{C}}$ are the angles between $O_2\hat{B}$ and $O_2\hat{C}$ and O_2H. These two angles will change with the rotation of the circular pulley. θ_B and θ_C are the angles between O_2B and O_2C and O_2H as introduced before.

Following [11], the stretched lengths of the free spans $\widetilde{A}\widetilde{B}$ and $\widetilde{C}\widetilde{D}$ can be calculated from their unstretched lengths by

$$L_{\widetilde{A}\widetilde{B}} = (n_4 - 2)p_b \left(1 + \frac{F_{n+1}}{EA}\right) + p_{1,n_1} + p_{2,n_2} \tag{2.2.15}$$

$$L_{\widetilde{C}\widetilde{D}} = n_3 p_b \left(1 + \frac{F_0}{EA}\right) \tag{2.2.16}$$

$L_{\widetilde{A}\widetilde{B}}$ and $L_{\widetilde{C}\widetilde{D}}$ are the another expressions for the stretched lengths of spans $\widetilde{A}\widetilde{B}$ and $\widetilde{C}\widetilde{D}$. n_4 and n_3 are the numbers of belt pitch included in spans $\widetilde{A}\widetilde{B}$ and $\widetilde{C}\widetilde{D}$. EA is the belt longitudinal stiffness. F_{n+1} and F_0 are the belt tensions in the free spans AB and CD. p_b

is the unstretched length of one belt pitch. p_{1,n_1} is the stretched length of the belt pitch between the belt teeth n_1 and n_1+1; p_{2,n_2} is the stretched length of the belt pitch between the belt teeth n_2 and n_2+1. Belt teeth n_1+1 and n_2+1 are the teeth following n_1 and n_2. p_{1,n_1} and p_{2,n_2} can be expressed by

$$p_{1,n_1} = p_b\left(1+\frac{F_{1,n_1}}{EA}\right) + p_b\left(1+\frac{F'_{1,n_1}}{EA}\right) \tag{2.2.17}$$

$$p_{2,n_2} = p_b\left(1+\frac{F_{2,n_2}}{EA}\right) + p_b\left(1+\frac{F'_{2,n_2}}{EA}\right) \tag{2.2.18}$$

To calculate the free-span tensions, tooth contacts at the boundary region of the free span should be investigated. A pulley tooth is meshed when its centerline passes through tangent points from the spans AB or CD to the spans BC or AD. Situation is more complex for the belt tooth. As shown in Figure 2.11, pulley tooth i ($i \geq 1$) is in the meshed area and the pulley tooth 0 is out of the meshed area. Here, n represents the last tooth in the meshed area and n can be regarded as n_1 or n_2. For the first belt tooth, when the belt tooth 1 contacts with the pulley tooth 1 ($u_{j,1} > 0$), load condition for belt tooth 1 is the same as other meshed belt teeth and $F_0 = F_{j,1} - Q_{j,1}$. When the belt tooth 1 "contacts" with the pulley tooth 0 ($u_{j,1} < 0$), $Q_{j,1}$ equals to 0, and F_0 equals to $F_{j,1}$ due to the fact that the pulley tooth 0 is already out of contact.

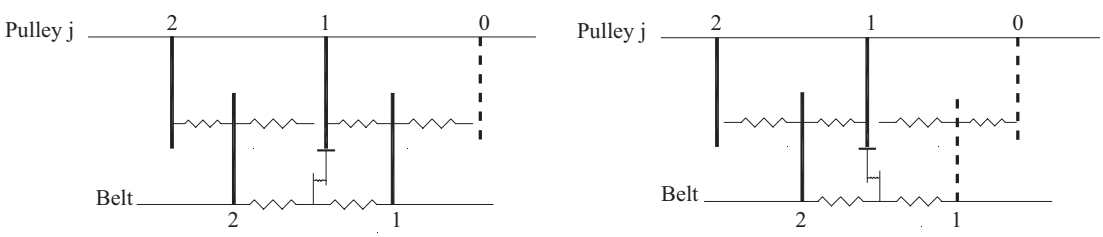

(a) $u_{j,1} > 0$ (b) $u_{j,1} < 0$

Figure 2.11: Loading conditions for the first belt tooth in contact. The thick solid lines denote the engaged belt teeth and pulley teeth. The thick dashed lines denote the disengaged belt teeth and pulley teeth. Both solid lines and dashed lines coincide with the teeth centerlines.

In Figure 2.12 , pulley tooth i ($i \leq n$) is in the meshed area and pulley tooth $n+1$ is out of

the meshed area. n still represents the last meshed tooth. When belt tooth $n+1$ "contacts" with the pulley tooth n+1 ($u_{j,n+1} > 0$), the tooth load $Q_{j,n+1}$ is zero, and the free-span tension F_{n+1} equals to F'_n. When the belt tooth $n+1$ contacts with the pulley tooth n ($u_{j,n+1} < 0$), tooth load $Q_{j,n+1}$ is not zero, and $F_{j,n+1} = Q_{j,n+1} + F'_{j,n}$.

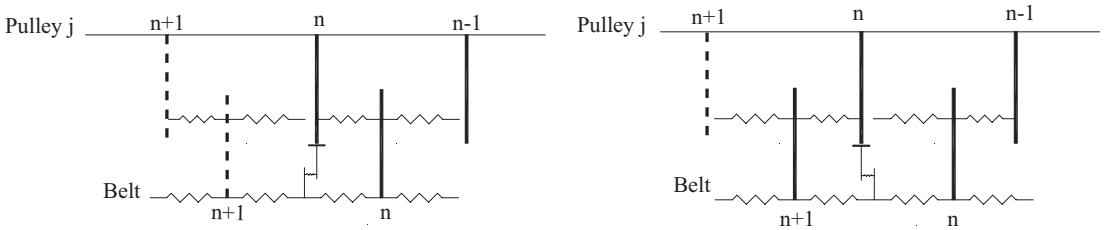

(a) $u_{j,n+1} > 0$ (b) $u_{j,n+1} < 0$

Figure 2.12: Loading conditions for the last belt tooth in contact. The thick solid lines denote the engaged belt teeth and pulley teeth. The thick dashed lines denote the disengaged belt teeth and pulley teeth. Both solid lines and dashed lines coincide with the teeth centerlines.

From the above discussion, two expressions l_b and L_b can be got for the stretched length of the total pitch line. One is from Figure 2.6 and the other one is from the sum of stretched lengths of the four spans $\widetilde{A}\widetilde{B}$, $\widetilde{C}\widetilde{D}$, $\widetilde{B}\widetilde{C}$, $\widetilde{A}\widetilde{D}$.

$$l_b = l_{AB} + l_{BC} + l_{CD} + l_{AD} \tag{2.2.19}$$

$$L_b = L_{\widetilde{A}\widetilde{B}} + L_{\widetilde{B}\widetilde{C}} + L_{\widetilde{C}\widetilde{D}} + L_{\widetilde{A}\widetilde{D}} \tag{2.2.20}$$

The lengths l_{AD} and l_{BC} of the span AD and the span BC in Figure 2.6 can be calculated by arclength formula 2.2.5 as

$$l_{AD} = R_1 (\theta_D - \theta_A) + (\varepsilon/4)(sin2\theta_D - sin2\theta_A) \tag{2.2.21}$$

$$l_{BC} = R_2 [2\pi - (\theta_C - \theta_B)] \tag{2.2.22}$$

The stretched lengths $L_{\widetilde{B}\widetilde{C}}$ and $L_{\widetilde{A}\widetilde{D}}$ of the spans $\widetilde{B}\widetilde{C}$ and $\widetilde{A}\widetilde{D}$ can be calculated according

to the system model in Section 2.1 as

$$L_{\widetilde{AD}} = \sum_{i=1}^{n_1} p_b + u_{1,i+1} - u_{1,i} \tag{2.2.23}$$

$$L_{\widetilde{BC}} = \sum_{i=1}^{n_2} p_b + u_{2,i+1} - u_{2,i} \tag{2.2.24}$$

Finally, two compatibility conditions have been found for the two-pulley timing belt system with an oval pulley.

$$l_b = L_b \tag{2.2.25}$$

$$l_{\widetilde{CD}} = L_{\widetilde{CD}} \tag{2.2.26}$$

Physically, the compatibility conditions guarantee that the same timing belt is used and there is only one unique condition of the belt tension distributions in one state. In addition, $l_{\widetilde{AD}} = L_{\widetilde{AD}}$ can be used to replace the compatibility condition 2.2.26.

2.2.2 Reference state

The loading conditions in the reference state will be determined after the installation of timing belt. When the properties of belt pitches are the same, tensions in the free spans are determined by two things: one is the elongation of each belt pitch and the other one is the number of belt pitch included.

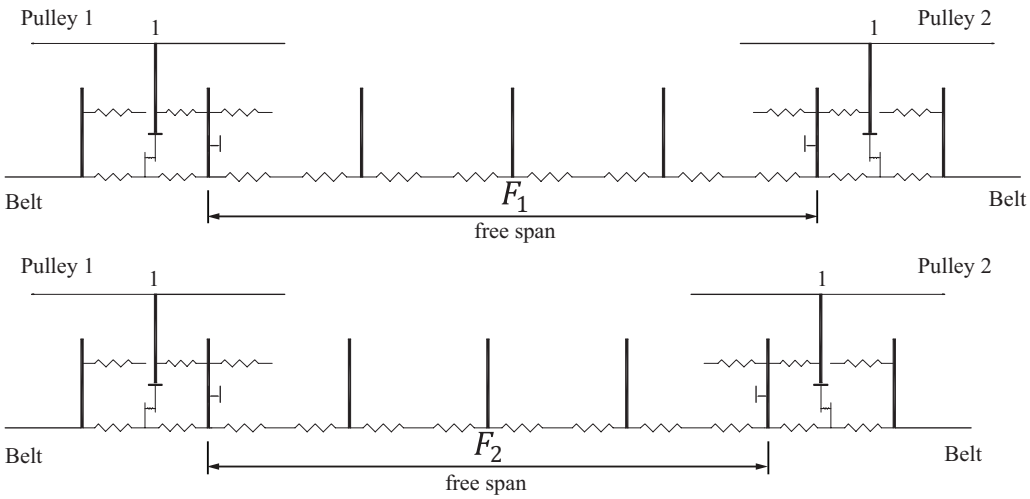

(a) Influence of belt pitch elongations

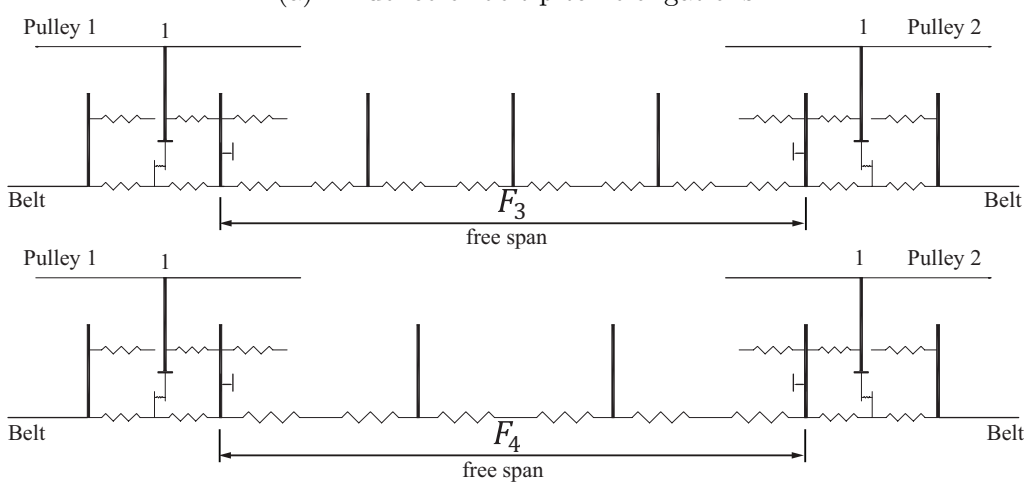

(b) Influence of belt pitch numbers

Figure 2.13: Sketches showing the influences of belt pitch numbers and belt pitch elongations on the free-span tensions

Two examples as Figure 2.13a and Figure 2.13b are used to introduce the impact of the two values. The influence of each belt pitch elongation is revealed in Figure 2.13a. When the belt pitch numbers included in two free spans are both four, the larger elongation of each belt pitch will lead to the larger tension in the free span. Therefore, the free-span tension F_1 is larger than F_2. For the belt pitch number, when the stretched lengths of two free spans are the same, larger belt pitch number included will result in the smaller free-span tension.

Therefore, the free-span tension F_4 is larger than F_3, as shown in Figure 2.13b.

Many factors can affect these two values, such as center distance between two pulleys, etc. Most of these factors can be analyzed in previous study. Only the influence of the pulley tooth is considered in this paper, which cannot be just handled by the pitch profile of the timing belt system. The positions of pulley teeth at the boundary of free spans can affect the free-span tensions because they determine the range of the free-span stretched lengths by restricting the movement of the meshed belt teeth. The Orientation of the pulley and the tooth distribution along the pulley determine the pulley configuration. Orientation angle is represented by γ and tooth distribution angle is represented by β. These two angles are constant for a pulley. For the oval pulley, as shown in Figure 2.14, $\{\mathbf{e_{1,1}}, \mathbf{e_{1,2}}\}$ and $\{\mathbf{E_{1,1}}, \mathbf{E_{1,2}}\}$ are the rotational reference frame and the fixed reference frame with the reference point at the center of the oval pulley. $\mathbf{E_{1,1}}$ is parallel to the centerline that connects the centers of the oval pulley and the circular pulley. The orientation angle γ_1 is from the axis $\mathbf{e_{1,1}}$ to the semi-major axis of the oval pulley. The tooth distribution angle β_1 is from the semi-major axis to the nearest tooth axis. The nearest tooth axis of the oval pulley is from the center of the oval pulley and passes through the intersection point between the pitch oval and the centerline of the pulley tooth that nearest to the semi-major axis (The tooth that is passed through by the nearest tooth axis is included) in the counterclockwise direction. α_1, from the axis $\mathbf{E_{1,1}}$ to the axis $\mathbf{e_{1,1}}$, is the rotation angle of the oval pulley for the arbitrary state.

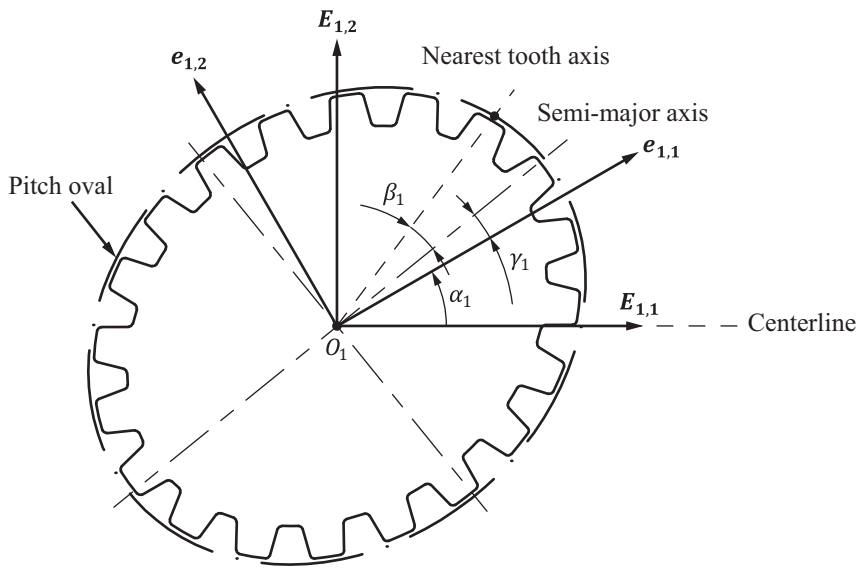

Figure 2.14: Orientation angle and tooth position angle of an oval pulley. $\{\mathbf{e_{1,1}}, \mathbf{e_{1,2}}\}$ is the rotational reference frame with respect to O_1. $\{\mathbf{E_{1,1}}, \mathbf{E_{1,2}}\}$ is the fixed reference frame with respect to O_1. $\mathbf{E_{1,1}}$ is parallel to the centerline that connects the centers of the oval pulley and the circular pulley. Nearest tooth axis is from O_1 to the intersection point of the pitch oval and the centerline of the pulley tooth that nearest to the semi-major axis in the counterclockwise direction.

For the circular pulley, as shown in Figure 2.15, $\{\mathbf{e_{2,1}}, \mathbf{e_{2,2}}\}$ and $\{\mathbf{E_{2,1}}, \mathbf{E_{2,2}}\}$ are the rotational reference frame and the fixed reference frame with the reference point at the center of the circular pulley. $\mathbf{E_{2,1}}$ is parallel to the centerline that connects the centers of the oval pulley and the circular pulley. Due to the symmetry of the circular pulley, the orientation angle for the circular pulley is meaningless. Therefore, only tooth distribution angle is defined. The tooth distribution angle β_2 is from the axis $\mathbf{e_{2,1}}$ to the nearest tooth axis. The nearest tooth axis of the circular pulley is from the center of the circular pulley and passes through the intersection point of the pitch circle and the centerline of the pulley tooth that nearest to the axis $\mathbf{e_{2,1}}$ (The tooth that is passed through by the nearest tooth axis is included) in the counterclockwise direction. α_2, from the axis $\mathbf{E_{2,1}}$ to the axis $\mathbf{e_{2,1}}$, is the rotation angle of the circular pulley for the arbitrary state.

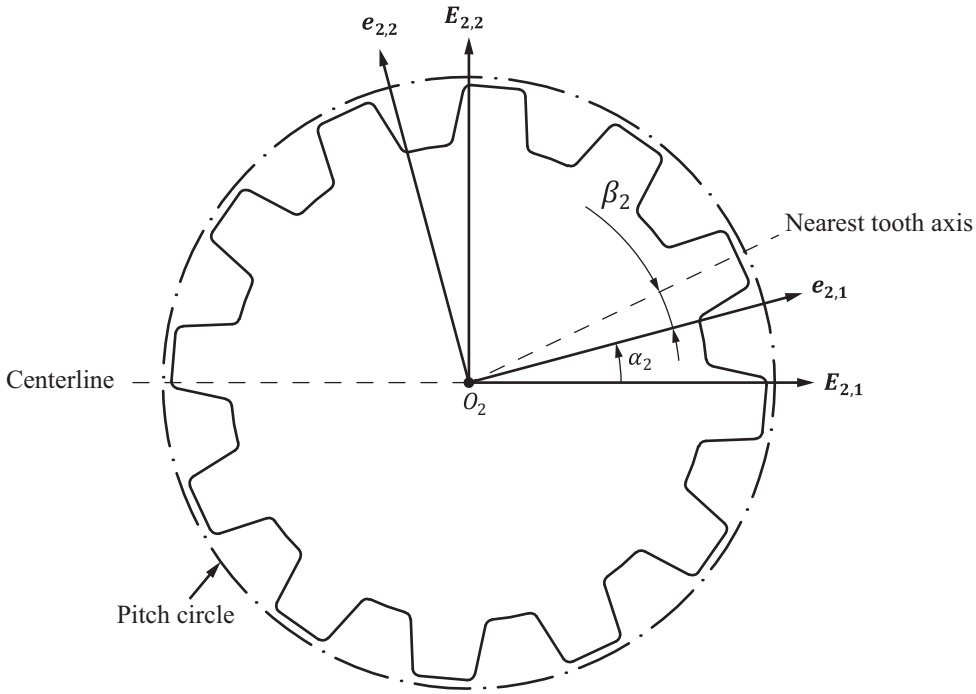

Figure 2.15: Orientation angle and tooth position angle of a circular pulley. $\{\mathbf{e_{2,1}}, \mathbf{e_{2,2}}\}$ is the rotational reference frame with respect to O_2. $\{\mathbf{E_{2,1}}, \mathbf{E_{2,2}}\}$ is the fixed reference frame with respect to O_2. $\mathbf{E_{2,1}}$ is parallel to the centerline that connects the centers of the oval pulley and the circular pulley. Nearest tooth axis is from O_2 to the intersection point of the pitch circle and the centerline of the pulley tooth that nearest to the axis $\mathbf{e_{2,1}}$ in the counterclockwise direction.

With certain pulley pitch p_p, these two angles can determine the positions of all the pulley teeth. Therefore, the orientation angles and the tooth distribution angles should be specified to determine the configurations of the pulleys. When these two angles are given, the process of calculating tension distributions for the reference state has almost no difference with that for the arbitrary state (introduced later). The only difference is that all the forces and deflections of teeth are assumed to be zero for the previous step before the reference state (the operation of the system is pursued step by step). Most of time, not both two angles will be specified for each pulley. Some other requests are added instead. Practically, when the orientation angles of both pulleys are equal to zero and the tooth distribution angle of the oval pulley is zero, the tensions in two free spans are required to be equal. Under this circumstance, it is important to calculate the tooth distribution angle for the circular pulley

by the newly added conditions. The problem becomes solving the tooth distribution angle for the circular pulley and the value of the equivalent tensions in two free spans.

To find the tension distribution in the timing belts and the tooth distribution around the circular pulley in the reference state, an iteration method is used. The flow chart on Figure 2.16 better illustrates the computation process. Following [5], the deflections of the belt teeth $u_{1,1}$ and $u_{2,1}$ meshed with the oval pulley and the circular pulley respectively should be determined by free-span tensions F_0 and F_{n+1}. Positions of these two belt teeth are indicated on Figure 2.1. Therefore, for the reference state, there are four unknowns $F_0(0)$, β_2, $u_{1,1}(0)$ and $u_{2,1}(0)$. $F_{n+1}(0)$ is not regarded as an additional unknown value because the value of $F_{n+1}(0)$ is the same as $F_0(0)$. Here, 0 in the parenthesis represents the reference state. Two big iteration loops are needed. The first one is to seek the value of equivalent free-span tensions and the second one is to determine the tooth distribution angle of the circular pulley. Among them, the first big iteration loop contains two small iteration loops to find the solutions of $u_{1,1}(0)$ and $u_{2,1}(0)$.

For the first big iteration loop, the iteration starts from the free span CD. In the reference state, the tension $F_0(0)$ in free span CD and the deflections of the first belt teeth $u_{1,1}(0)$ and $u_{2,1}(0)$ meshed with the oval pulley and the circular pulley respectively are assigned initial guesses

$$F_0\,(0) = f_0 \tag{2.2.27}$$

$$u_{1,1}(0) = u_{1,1\_0} \tag{2.2.28}$$

$$u_{2,1}(0) = u_{2,1\_0} \tag{2.2.29}$$

From Equation 2.1.4, if $u_{1,1\_0} > 0$, $Q_{1,1}(0)$ can be got by multiplying $u_{1,1\_0}$ and c_z; if $0 \geq u_{1,1\_0} \geq -b$, $Q_{1,1}(0)$=0; if $-b > u_{1,1\_0}$, $Q_{1,1}(0)$ equals to $(u_{1,1\_0} + b)c_z$. $F_{1,1}(0)$ can then be calculated by substituting $Q_{1,1}(0)$ into Equation 2.1.3.

$$F_{1,1}(0) = Q_{1,1}(0) + F'_{1,0}(0) \tag{2.2.30}$$

where $F'_{1,0}(0)$ is the same as the free-span tension and equals to f_0. As mentioned before, the deflection of the first meshed belt tooth $u_{1,1}(0^*)$, tension force $F_{1,1}(0^*)$, and the deflection of the belt pitch mid-point $v_{1,1}(0^*)$ before the reference state are assumed to be zero. 0^* represents the preceding step before the reference state. Equation 2.1.12 then gives the deflection of the belt pitch mid-point $v_{1,1}(0)$ for the reference state

$$\begin{aligned} v_{1,1}(0) &= u_{1,1}(0) - u_{1,1}(0^*) + \frac{F_{1,1}(0) - F_{1,1}(0^*)}{2c_R} + v_{1,1}(0^*) \\ &= u_{1,1}(0) + \frac{F_{1,1}(0)}{2c_R} \end{aligned} \tag{2.2.31}$$

Using Equation 2.1.6, friction force $R_{1,1}(0)$ between the top lands of the first oval pulley tooth and the belt groove is

$$R_{1,1}(0) = v_{1,1}(0)c_f \tag{2.2.32}$$

Tension $F'_{1,1}(0)$ can be got from the Equation 2.1.5 with $R_{1,1}(0)$ and $F_{1,1}(0)$

$$F'_{1,1}(0) = F_{1,1}(0) + R_{1,1}(0) \tag{2.2.33}$$

The deflection of the second belt tooth meshed with the oval pulley can then be calculated using Equation 2.1.8

$$u_{1,2}(0) = u_{1,1}(0) + \frac{F_{1,1}(0) + F'_{1,1}(0)}{2c_R} \tag{2.2.34}$$

Through repeated process, the tension $F_{1,n_1+1}(0)$ in the free span AB can be finally calculated from the part of belt meshed with the oval pulley, and the tension $F_{2,n_2+1}(0)$ in the free span AB calculated from the part of belt meshed with the circular pulley can also be got by similar method.

Because the tension $F_{n+1}(0)$ in the free span AB is equal to the tension $F_0(0)$ in the free span CD, $F_{1,n_1+1}(0)$ and $F_{2,n_2+1}(0)$ are compared with $F_0(0)$ to determine the true value of $u_{1,1}(0)$ and $u_{2,1}(0)$. If $F_{1,n_1+1}(0) < F_0(0)$, $u_{1,1\_0}$ is less than the true value of $u_{1,1}(0)$ and should be increased. If $F_{1,n_1+1}(0) > F_0(0)$, $u_{1,1\_0}$ is larger than the true value of $u_{1,1}(0)$ and

should be decreased. The solution of $u_{1,1\_0}$ can be determined until the difference between $F_{1,n_1+1}(0)$ and $F_0(0)$ is small enough. In this study, $F_{1,n_1+1}(0)$ and $F_0(0)$ converge when $|[F_{1,n_1+1}(0)-F_0(0)]/F_0(0)| < 0.1\%$. The process is similar for the $u_{2,1\_0}$. If $F_{2,n_2+1}(0) < F_0(0)$, $u_{2,1\_0}$ should be increased, and if $F_{2,n_2+1}(0) > F_0(0)$, $u_{2,1\_0}$ should be decreased. $F_{2,n_2+1}(0)$ and $F_0(0)$ converge when $|[F_{2,n_2+1}(0) - F_0(0)]/F_0(0)| < 0.1\%$. After $u_{1,1}(0)$ and $u_{2,1}(0)$ are determined, tension distributions in belts $(F_{1,i}(0), F'_{1,i}(0), F_{2,i}(0), F'_{2,i}(0))$, deflections of belt teeth $(u_{1,i}(0), u_{2,i}(0))$, and friction forces between pulley teeth top and belt groove $(R_{1,i}(0), R_{2,i}(0))$ can all be determined based on the initial guess of the tension in the free span CD.

To find the tension in the free span CD, the first compatibility condition 2.2.25 is used. In Equation 2.2.25, $l_b(0)$ can be calculated by the coordinates of points A, B, C and D as introduced in section 2.2.1 and will not be affected by the tension distribution in timing belts. On the contrary, different tension distributions in timing belts will result in different $L_b(0)$. Considering the initial guess of the tension in the free span CD, Equations 2.2.15, 2.2.16, 2.2.23 and 2.2.24 give

$$L_{\widetilde{A}\widetilde{B}}(0) = [n_4(0) - 2]p_b \left[1 + \frac{F_{n+1}(0)}{EA}\right] + p_{1,n_1}(0) + p_{2,n_2}(0) \tag{2.2.35}$$

$$L_{\widetilde{C}\widetilde{D}}(0) = n_3(0)p_b \left[1 + \frac{F_0(0)}{EA}\right] \tag{2.2.36}$$

$$L_{\widetilde{A}\widetilde{D}}(0) = \sum_{i=1}^{n_1} p_b + u_{1,i+1}(0) - u_{1,i}(0) \tag{2.2.37}$$

$$L_{\widetilde{B}\widetilde{C}}(0) = \sum_{i=1}^{n_2} p_b + u_{2,i+1}(0) - u_{2,i}(0) \tag{2.2.38}$$

In these equations, $F_{n+1}(0)$ equals to $F_0(0)$, and both of them are assigned initial guesses f_0. $n_3(0)$ and $n_4(0)$ are the belt pitch numbers included in the spans $\widetilde{C}\widetilde{D}$ and $\widetilde{A}\widetilde{B}$ for the reference state, which should be specified during the installation. p_b is the unstretched length of one belt pitch. $p_{1,n_1}(0)$ is the stretched length of the belt pitch between belt teeth n_1 and

$n_1 + 1$; $p_{2,n_2}(0)$ is the stretched length of the belt pitch between belt teeth n_2 and $n_2 + 1$. They can be calculated by Equations 2.2.17 and 2.2.18 as

$$p_{1,n_1}(0) = p_b \left[1 + \frac{F_{1,n_1}(0)}{EA}\right] + p_b \left[1 + \frac{F'_{1,n_1}(0)}{EA}\right] \tag{2.2.39}$$

$$p_{2,n_2}(0) = p_b \left[1 + \frac{F_{2,n_2}(0)}{EA}\right] + p_b \left[1 + \frac{F'_{2,n_2}(0)}{EA}\right] \tag{2.2.40}$$

L_b can finally be got by the substitution of Equations 2.2.35, 2.2.36, 2.2.37, 2.2.38 into Equation 2.2.20. Physically, if $l_b(0) > L_b(0)$, the assumed f_0 is smaller than the true $F_0(0)$ and should be increased in the next iteration step; if $l_b(0) < L_b(0)$, the assumed f_0 is larger than the true $F_0(0)$ and should be decreased in the next iteration step. In this study, $l_b(0)$ and $L_b(0)$ converge when $|[l_b(0) - L_b(0)]/l_b(0)| < 0.001\%$. The limit value of the error between lengths are smaller than the limit value of the error between forces in this study because the stiffness of the timing belt is large, which will tremendously increase the error between forces from a small error between lengths.

For the second big iteration loop, the unknown tooth distribution angle β_2 of the circular pulley is first assigned an initial guess

$$\beta_2 = \beta_{2\_0} \tag{2.2.41}$$

The stretched length $l_{\widetilde{C}\widetilde{D}}(0)$ of span $\widetilde{C}\widetilde{D}$ can be calculated from Equation 2.2.7

$$l_{\widetilde{C}\widetilde{D}}(0) = l_{CD}(0) + d_C(0) + d_D(0) - 2d_w + u_{1,1}(0) + u_{2,1}(0) \tag{2.2.42}$$

l_{CD} are the stretched length of the span CD as shown in Figure 2.6 and can be calculated from Equation 2.2.9. $u_{1,1}(0)$ and $u_{2,1}(0)$ are the deflections of the first belt teeth meshed with the oval pulley and the circular pulley respectively. These two values are the results calculated from the first big iteration loop. d_w is the unstretched length between two centerlines of a pair of meshed pulley tooth and belt tooth and can be got from $(p_p - b)/2$. $d_C(0)$ and $d_D(0)$

are the distances between tangent points C and D and intersection points $\hat{C}$ and $\hat{D}$ in the reference state and can be calculated from Equations 2.2.14 and 2.2.12. In these equations, $\theta_{\hat{D}}(0)$ can be determined physically by $\theta_D(0)$ and β_1 (β_1 is the tooth distribution angle of the oval pulley and $\beta_1 = 0$); $\theta_{\hat{C}}(0)$ is determined physically by $\theta_C(0)$ and β_{2_0}. For example, for $\theta_{\hat{D}}(0)$,

$$\theta_D(0) - \tau < \theta_{\hat{D}}(0) < \theta_D(0) \tag{2.2.43}$$

where τ is the wrap angle of one belt pitch. There is only one unique value of $\theta_{\hat{D}}(0)$ in this range, and the unique $\theta_{\hat{D}}(0)$ can be determined as $\beta_1 = 0$.

To find the value of β_{2_0}, the compatibility condition 2.2.26 is checked. Compare the value of $l_{\widetilde{C}\widetilde{D}}(0)$ from Equation 2.2.42 and $L_{\widetilde{C}\widetilde{D}}(0)$ from Equation 2.2.36. If $l_{\widetilde{C}\widetilde{D}}(0)$ is larger than $L_{\widetilde{C}\widetilde{D}}(0)$, β_{2_0} should be decreased in the next iteration step; if $l_{\widetilde{C}\widetilde{D}}(0)$ is smaller than $L_{\widetilde{C}\widetilde{D}}(0)$, β_{2_0} should be increased in the next iteration step. In this study, the results converge when $|[L_{\widetilde{C}\widetilde{D}}(0) - l_{\widetilde{C}\widetilde{D}}(0)]/L_{\widetilde{C}\widetilde{D}}(0)| < 0.001\%$. At last, tension distributions in timing belts and the tooth distribution angle of the circular pulley in the reference state are both found, which will be used to further calculate the tension distributions of the system in the arbitrary state.

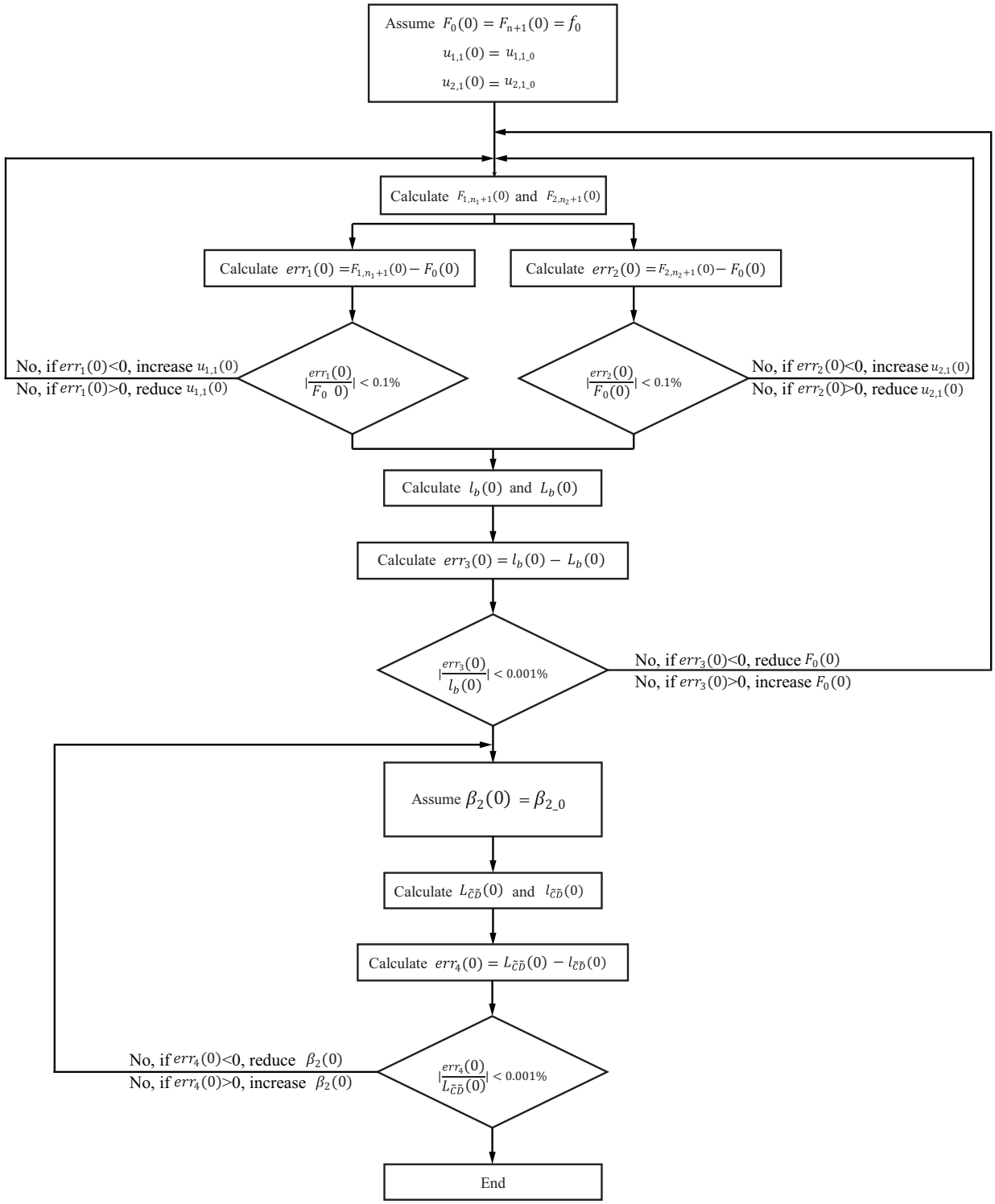

Figure 2.16: Computation process of the belt tension distributions for the two-pulley timing belt system with an oval pulley in the reference state.

2.2.3 Arbitrary state

For a two-pulley system with an oval pulley, timing belts are used to precisely synchronize the rotation of the oval pulley and the circular pulley, which means the oval pulley and the circular pulley in this system have the same linear velocity. As introduced in Equation 2.2.1, the oval pulley has an imaginary equivalent circular pulley that has the same circumference as the oval pulley and has an equivalent radius R_1. Therefore, for an ideal two-pulley timing belt system, the rotation relationship between the oval pulley and the circular pulley is

$$\frac{\alpha_1}{\alpha_2} = \frac{R_2}{R_1} \tag{2.2.44}$$

where α_1 is the rotation angle of the oval pulley, α_2 is the rotation angle of the circular pulley, R_1 is the equivalent radius of the oval pulley and R_2 is the radius of the circular pulley. For convenience, α is used to represent the arbitrary state in this paper.

Due to the change of the tooth numbers n_1 and n_2 in the spans $\widetilde{A}\widetilde{D}$ and $\widetilde{B}\widetilde{C}$, and the change of the belt pitch numbers n_4 and n_3 in the spans $\widetilde{A}\widetilde{B}$ and $\widetilde{C}\widetilde{D}$, load distributions for the arbitrary state are affected by the load conditions in the preceding step (the rotation of the pulleys are pursued step by step in this work as mentioned before). To find the relations between the tooth numbers and the belt pitch numbers in two adjacent steps respectively, rotation angle of each step needs to be chosen after deliberate consideration. Large rotation angle will miss the number change and small rotation angle will increase the computation time. Rotation angle of one step is chosen as the central angle subtended by one circular pulley pitch (p_p/R_2) in this paper, which can monitor every tooth number change and every belt pitch number change in the corresponding spans at a high calculating speed. When pulleys rotate counterclockwise, the tooth numbers in the spans $\widetilde{A}\widetilde{D}$ and $\widetilde{B}\widetilde{C}$ and the belt pitch numbers in the spans $\widetilde{A}\widetilde{B}$ and $\widetilde{C}\widetilde{D}$ can be determined by the rules: if $d_A(\alpha) < d_A(\alpha^*)$, $n_1(\alpha) = n_1(\alpha^*) + 1$, and $n_4(\alpha) = n_4(\alpha^*) - 1$; if $d_B(\alpha) > d_B(\alpha^*)$, $n_4(\alpha) = n_4(\alpha^*) + 1$, and $n_2(\alpha) = n_2(\alpha^*) - 1$; if $d_C(\alpha) > d_C(\alpha^*)$, $n_2(\alpha) = n_2(\alpha^*) - 1$, and $n_3(\alpha) = n_3(\alpha^*) + 1$; if $d_D(\alpha) < d_D(\alpha^*)$, $n_1(\alpha) = n_1(\alpha^*) + 1$, and $n_3(\alpha) = n_3(\alpha^*) - 1$; α^* represents the previous

step before the current state α. The starting value of n_1, n_2, n_3 and n_4 have already been specified during the installation. After the relations between the tooth numbers and the belt pitch numbers in two adjacent states, the tooth distribution angle of the circular pulley, and the tension distributions in the reference state are determined, a computational procedure is set up to calculate the load distribution at an arbitrary pulley rotation angle. A flow chart below displays the technical details.

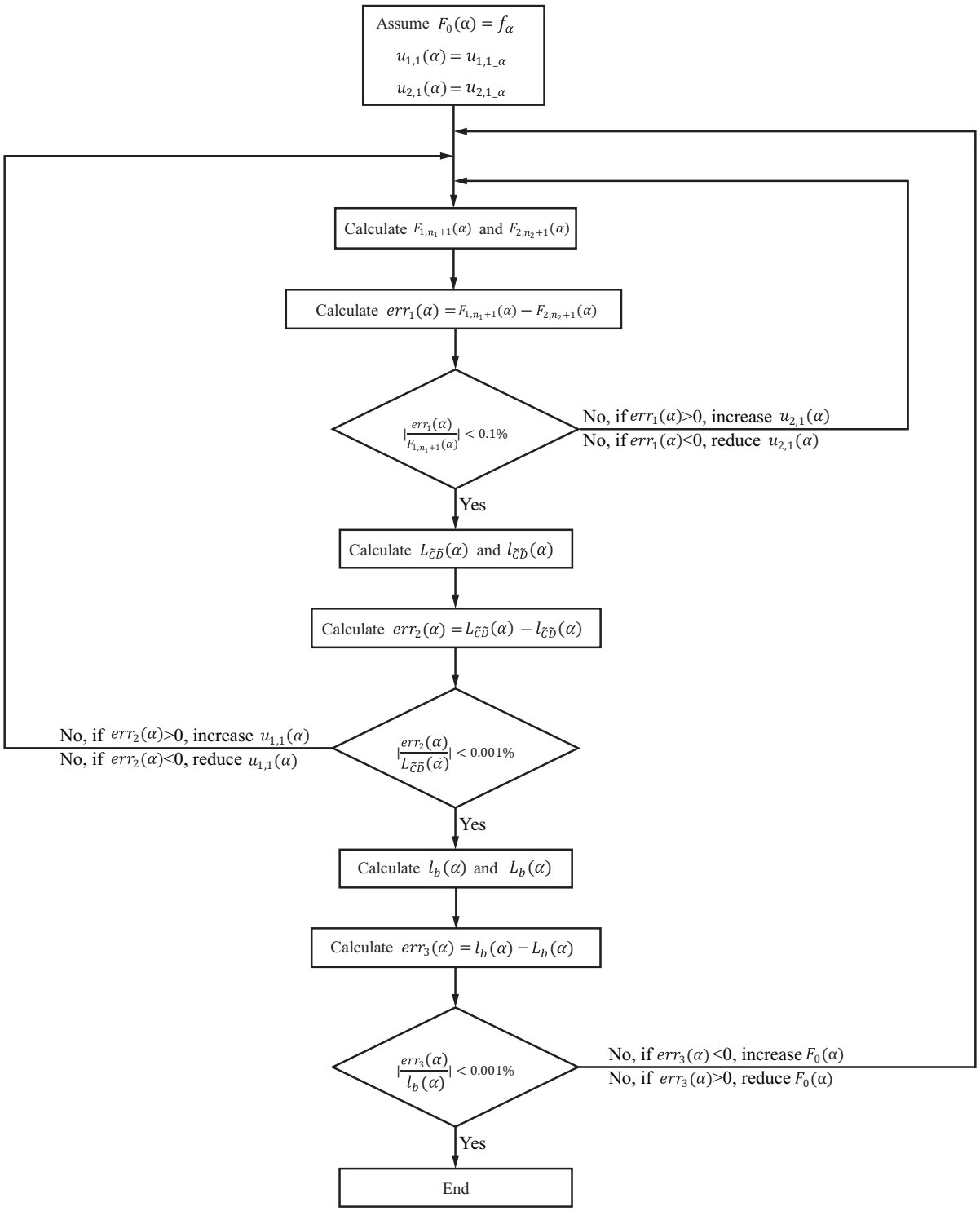

Figure 2.17: Computation process of the belt tension distributions for the two-pulley timing belt system with an oval pulley in the arbitrary state

In this problem, belt tensions in the free span AB and CD, the deflection $u_{1,1}(\alpha)$ of the first belt tooth meshed with the oval pulley and the deflection $u_{2,1}(\alpha)$ of the first belt tooth meshed with the circular pulley are unknown for the arbitrary state. To find them, a modified iteration method is used. The iteration still starts from the free span CD. The tension $F_0(\alpha)$ in the free span CD, deflections $u_{1,1}(\alpha)$ and $u_{2,1}(\alpha)$ of the first belt tooth meshed with the oval pulley and the circular pulley respectively are assigned initial guesses

$$F_0\left(\alpha\right) = f_\alpha \tag{2.2.45}$$

$$u_{1,1}(\alpha) = u_{1,1\_\alpha} \tag{2.2.46}$$

$$u_{2,1}(\alpha) = u_{2,1\_\alpha} \tag{2.2.47}$$

Similar to the computation process of the reference state, Equation 2.1.4 is first used to calculate the tooth load $Q_{1,1}(\alpha)$ for the arbitrary state between the first oval pulley tooth and the corresponding belt tooth 1 in three different cases. Then substitution of $Q_{1,1}(\alpha)$ into Equation 2.1.3 yields

$$F_{1,1}(\alpha) = Q_{1,1}(\alpha) + F'_{1,0}(\alpha) \tag{2.2.48}$$

where $F_{1,1}(\alpha)$ is the tension in the first half belt pitch between the belt pitch mid-point and belt tooth 1 for the arbitrary state, and $F'_{1,0}(\alpha)$ is equal to the assumed tension $f_0(\alpha)$ in the free span CD. Deflection of the belt pitch mid-point $v_{1,1}(\alpha)$ in the arbitrary state can be calculated by Equation 2.1.12

$$v_{1,1}\left(\alpha\right) = u_{1,1}\left(\alpha\right) - u_{1,1}\left(\alpha^*\right) + \frac{F_{1,1}\left(\alpha\right) - F_{1,1}\left(\alpha^*\right)}{2c_R} + v_{1,1}\left(\alpha^*\right) \tag{2.2.49}$$

where $u_{1,1}(\alpha^*)$, $F_{1,1}(\alpha^*)$, and $v_{1,1}(\alpha^*)$ are the tooth deflection, the belt tension and the belt pitch mid-point deflection in the preceding step α^*. Because $u_{1,1}(0)$, $F_{1,1}(0)$, $v_{1,1}(0)$ of the reference state are the only known values before the arbitrary state, all the calculation for any arbitrary state should start from the reference state step by step. When $v_{1,1}(\alpha)$ is found,

Equation 2.1.6 gives the friction force $R_{1,1}(\alpha)$ for the arbitrary state

$$R_{1,1}(\alpha) = v_{1,1}(\alpha)c_f \tag{2.2.50}$$

$R_{1,1}(\alpha)$ is then used in Equation 2.1.5 to calculate the tension $F'_{1,1}(\alpha)$

$$F'_{1,1}(\alpha) = F_{1,1}(\alpha) + R_{1,1}(\alpha) \tag{2.2.51}$$

With these values, the deflection of the second belt tooth $u_{1,2}(\alpha)$ meshed with the oval pulley can be calculated by Equation 2.1.8 for the arbitrary state

$$u_{1,2}(\alpha) = u_{1,1}(\alpha) + \frac{F_{1,1}(\alpha) + F'_{1,1}(\alpha)}{2c_R} \tag{2.2.52}$$

In the end, the tension $F_{1,n_1+1}(\alpha)$ for the arbitrary state can be calculated from the belts meshed with the oval pulley. Through same process, the tension $F_{2,n_2+1}(\alpha)$ can also be calculated from the belts meshed with the circular pulley. These two values should be equal because they both represent the tension in the free span AB. Increase $u_{2,1}(\alpha)$, if $F_{1,n_1+1}(\alpha) > F_{2,n_2+1}(\alpha)$, and decrease $u_{2,1}(\alpha)$, if $F_{1,n_1+1}(\alpha) < F_{2,n_2+1}(\alpha)$. $F_{1,n_1+1}(\alpha)$ and $F_{2,n_2+1}(\alpha)$ converge when $|[F_{1,n_1+1}(\alpha) - F_{2,n_2+1}(\alpha)]/F_{1,n_1+1}(\alpha)| < 0.1\%$. The result of this iteration loop is to find the specific $u_{2,1}(\alpha)$ corresponding to initial guesses $u_{1,1\_\alpha}$ and f_α. At the same time, tension distributions in timing belts ($F_{1,i}(\alpha)$, $F'_{1,i}(\alpha)$, $F_{2,i}(\alpha)$, $F'_{2,i}(\alpha)$), deflections of belt teeth ($u_{1,i}(\alpha)$, $u_{2,i}(\alpha)$) and friction forces ($R_{1,i}(\alpha)$, $R_{2,i}(\alpha)$) are also determined for the arbitrary state by the initial guesses of $u_{1,1\_\alpha}$ and f_α.

To find the specific $u_{1,1}(\alpha)$ with respect to the initial guess f_α, the compatibility condition 2.2.26 is used. Equations 2.2.16 and 2.2.7 give two different methods to calculate the stretched length of the span $\widetilde{C}\widetilde{D}$

$$L_{\widetilde{C}\widetilde{D}}(\alpha) = n_3(\alpha)p_b\left[1 + \frac{F_0(\alpha)}{EA}\right] \tag{2.2.53}$$

$$l_{\widetilde{C}\widetilde{D}}(\alpha) = l_{CD}(\alpha) + d_C(\alpha) + d_D(\alpha) - 2d_w + u_{1,1}(\alpha) + u_{2,1}(\alpha) \tag{2.2.54}$$

l_{CD} can be solved by Equation 2.2.9. $d_C(\alpha)$ and $d_D(\alpha)$ can be solved by Equations 2.2.14 and 2.2.12. $F_0(\alpha)$, $u_{1,1}(\alpha)$, and $u_{2,1}(\alpha)$ are determined in the previous iteration step. $n_3(\alpha)$ can be calculated by the belt pitch number change relation. Compare $L_{\widetilde{C}\widetilde{D}}(\alpha)$ and $l_{\widetilde{C}\widetilde{D}}(\alpha)$ to adjust the value of the initial guess $u_{1,1\_\alpha}$. Increase $u_{1,1\_\alpha}$ when $L_{\widetilde{C}\widetilde{D}}(\alpha) > l_{\widetilde{C}\widetilde{D}}(\alpha)$, and decrease $u_{1,1\_\alpha}$ when $L_{\widetilde{C}\widetilde{D}}(\alpha) < l_{\widetilde{C}\widetilde{D}}(\alpha)$. $u_{1,1\_\alpha}$ reaches to its target value when $|[L_{\widetilde{C}\widetilde{D}}(\alpha) - l_{\widetilde{C}\widetilde{D}}(\alpha)]/L_{\widetilde{C}\widetilde{D}}(\alpha)| < 0.001\%$.

To find the true value of $F_0(\alpha)$, the compatibility condition 2.2.25 is used. $l_{AB}(\alpha)$, $l_{BC}(\alpha)$, $l_{CD}(\alpha)$, $l_{AD}(\alpha)$ can be calculated from the coordinates of tangent points in the arbitrary state and substitutions of these four values into Equation 2.2.19 yield $l_b(\alpha)$. Following Equations 2.2.15, 2.2.24, 2.2.16, 2.2.23, $L_{\widetilde{A}\widetilde{B}}(\alpha)$, $L_{\widetilde{B}\widetilde{C}}(\alpha)$, $L_{\widetilde{C}\widetilde{D}}(\alpha)$, $L_{\widetilde{A}\widetilde{D}}(\alpha)$ can be calculated for the arbitrary state and substitutions of these values into Equation 2.2.20 yield $L_b(\alpha)$. The compatibility condition 2.2.25 requests that $l_b(\alpha)$ should equal to $L_b(\alpha)$. To the end, $l_b(\alpha)$ and $L_b(\alpha)$ are compared. If $l_b(\alpha) > L_b(\alpha)$, f_α is smaller than the true value of $F_0(\alpha)$ and should be increased; if $l_b(\alpha) < L_b(\alpha)$, f_α is larger than the true value of $F_0(\alpha)$ and should be decreased. In this study, the results converge when $|[l_b(\alpha) - L_b(\alpha)]/l_b(\alpha)| < 0.001\%$.

Through the iteration method, tensions $F_{n+1}(\alpha)$ and $F_0(\alpha)$ in the free span AB and CD, tension distributions along the belt, deflections of belt teeth, and friction forces between pulley tooth top and belt groove can be determined for the arbitrary state and torque on pulley 2 in the arbitrary state can be calculated by

$$T(\alpha) = R_2[F_0(\alpha) - F_{n+1}(\alpha)] \tag{2.2.55}$$

The key point of iteration methods for the reference state and the arbitrary state is using two compatibility conditions to calculate the two unknown values caused by the oval pulley. These two compatibility conditions are interchangeable, which means no matter what compatibility condition is used to find the first unknown value, the other compatibility condition

has the ability to find the second unknown value. For the assumption that all the loads and the deflections before the reference state are assumed to be zero, it can affect the load distributions in both the reference state and the arbitrary state. However, the effects of this assumption on the load distributions are fading out with every step and the system becomes steady after around one revolution. Based on this assumption at the starting step, the load distributions of each following step can be calculated. The error caused by this assumption can be substantially reduced by replacing the assumed loads and deflections with the loads and the deflections calculated at the step right before the oval pulley overlaps itself that was in the reference state after the system is steady, and recalculating the load distributions with the new assumed loads and deflections.

2.3 Complex timing belt system

It is important to challenge a more complex system because two-pulley timing belt system with an oval pulley is the simplest timing belt drive system. First, a method to handle the problem of a two-pulley system with a special-shaped pulley will be presented. Second, load distributions of a three-pulley system with two oval pulleys will be analyzed. After the study of these two systems, loading conditions of multi-pulley systems with multiple customized pulleys can be obtained accordingly.

2.3.1 Two-pulley system with a special-shaped pulley

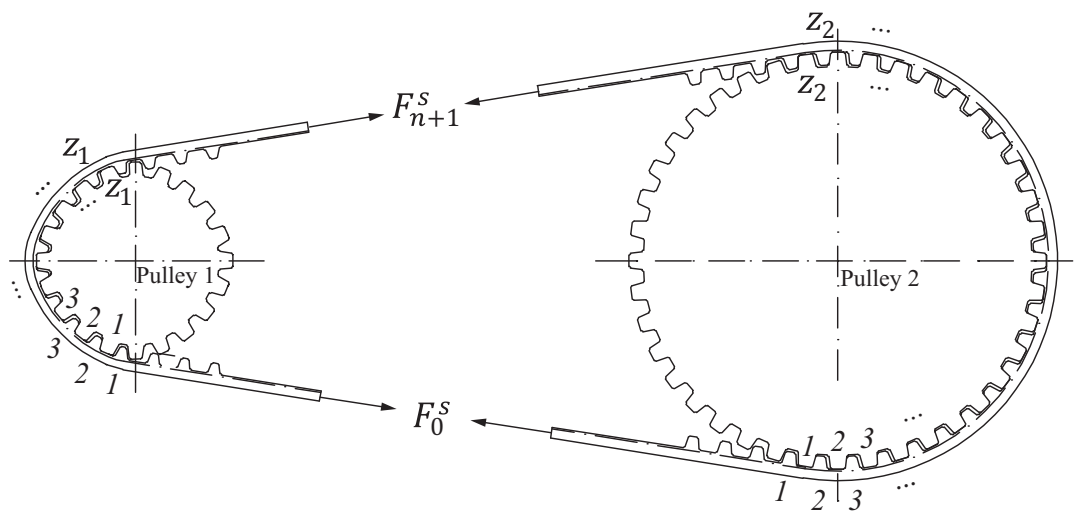

Figure 2.18: Teeth indexes of the two-pulley system with an inflated rounded square pulley.

An oval pulley can only provide a periodic torque with period π due to its geometric constraint. In practice, different periods of different torques are needed in different situations. To this end, research of the special-shaped pulley is necessary and a two-pulley system with an inflated rounded square pulley is investigated. Technically, the computation process of a system with a special-shaped pulley has almost no difference with that of a system with an oval pulley. The only difference is between the expression of the special-shaped pulley and that of an oval pulley. For the inflated rounded square pulley, the radius is defined as

$$R(\varphi) = R_1^s + (\varepsilon^s/2)\, cos4\varphi \tag{2.3.1}$$

R_1^s is the radius of an equivalent circular pulley. ε^s is the difference between the longest diameter of the square pulley and the diameter of the equivalent circular pulley. For convenience, inflated rounded square pulley are referred to as square pulley for the following introduction. The positions of pulley teeth and belt teeth are indexed as shown in Figure 2.18. z_1 and z_2 are the tooth number included in the meshed area. z_3 and z_4 are the belt pitch numbers in the spans $\widetilde{C}\widetilde{D}$ and $\widetilde{A}\widetilde{B}$. The pitch profile of the system is shown in Figure

2.19

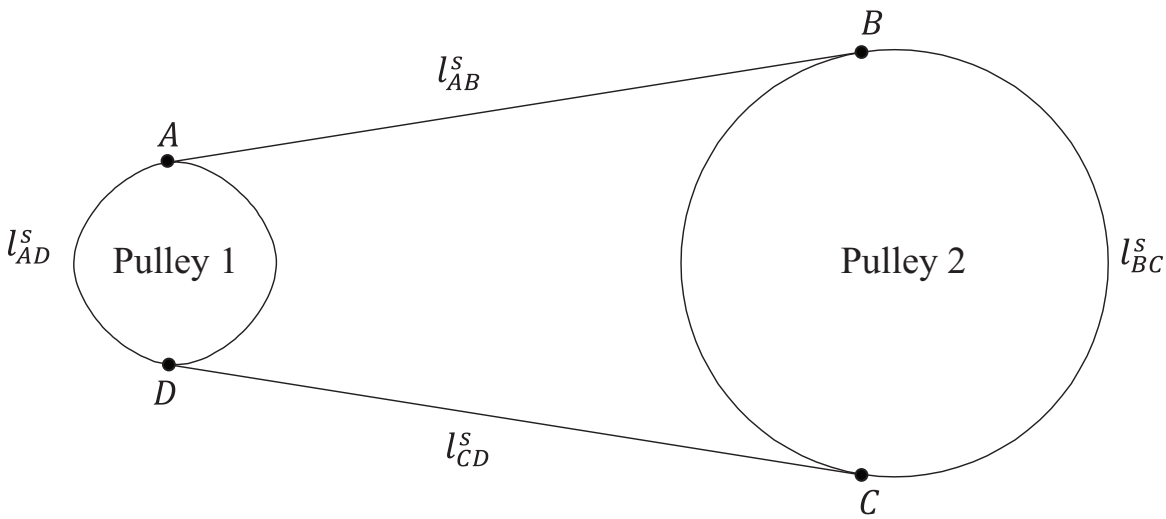

Figure 2.19: Pitch profile of the two-pulley system with an square pulley.

A, B, C, and D are the tangent points. l^s_{AB}, l^s_{BC}, l^s_{CD}, and l^s_{AD} are the stretched lengths of AB, BC, CD, and AD.

2.3.1.1 Reference state

Similarly, a square pulley will lead to two unknown free-span tensions for the timing belt system. One is the tension in the free span AB and the other one is the tension in the free span CD. In actual situation, another restriction will be added to the system. Two free-span tensions are required to be the same, when the long axis of the square pulley parallel to the centerline between the square pulley and the circular pulley. The long axis is the axis coincide with the longest radius of the square pulley. The tooth distribution angle of the square pulley is assumed to be zero, which means that there is a centerline of one pulley tooth coinciding with the long axis. The tooth distribution angle of the circular pulley then becomes the second unknown value.

An iteration method is used to determine the tension distributions in the timing belts and the tooth distribution angle of the circular pulley. Some calculations for the reference state

and the arbitrary state are completely the same as the two-pulley system with an oval pulley. These calculations are not repeated and only the necessary results are mentioned. Iteration starts from the free span CD. The tension in the free span CD, the deflection of the first belt tooth meshed with the square pulley, and the deflection of the first belt tooth meshed with the circular pulley are assigned initial guesses.

$$F_0^s(0) = f_0^s \tag{2.3.2}$$

$$u_{1,1}^s(0) = u_{1,1\_0}^s \tag{2.3.3}$$

$$u_{2,1}^s(0) = u_{2,1\_0}^s \tag{2.3.4}$$

Superscript s means the value belongs to the two-pulley timing belt system with a square pulley. Tooth load $Q_{1,1}^s(0)$, belt tension $F_{1,1}^s(0)$, friction force $R_{1,1}^s(0)$, and the deflection of the belt pitch mid-point $v_{1,1}^s(0)$ are calculated. Deflection of the second belt tooth meshed with the square pulley $u_{1,2}^s(0)$ can then be determined. Through repeated process, the tension $F_{1,z_1+1}^s(0)$ in the free span AB can be calculated from the part of belts meshed with the square pulley. In the meantime, the tension $F_{2,z_2+1}^s(0)$ in the free span AB can also be calculated from the part of belts meshed with the circular pulley. The initial guesses of the two belt teeth deflections are adjusted until the tensions calculated from the two belt parts converge such that $|[F_{1,z_1+1}^s(0) - F_0^s(0)]/F_0^s(0)| < 0.1\%$, and $|[F_{2,z_2+1}^s(0) - F_0^s(0)]/F_0^s(0)| < 0.1\%$. The compatibility condition about the stretched length of the total pitch line is checked based on the value determined from the previous iteration step. If $l_b^s(0)$ calculated from Equation 2.2.19 is larger than $L_b^s(0)$ calculated from Equation 2.2.20, the initial guess of the tension in the free span CD should be increased. Otherwise, if $l_b^s(0)$ is smaller than $L_b^s(0)$, the initial guess of the tension in the free span CD should be decreased. True values of the belt tension distributions, the deflections of the belt teeth, and the friction forces for the reference state are all found when $l_b^s(0)$ and $L_b^s(0)$ converge such that $|[l_b^s(0) - L_b^s(0)]/l_b^s(0)| < 0.001\%$.

An initial guess about the tooth distribution angle of the circular pulley is then assigned

$$\beta_2^s = \beta_{2\_0}^s \tag{2.3.5}$$

$l_{\widetilde{C}\widetilde{D}}^s$ and $L_{\widetilde{C}\widetilde{D}}^s$ (both represent the stretched length of the span $\widetilde{C}\widetilde{D}$) are calculated from Equations 2.2.7 and 2.2.16. The tooth distribution angle of the circular pulley β_2^s is adjusted by comparing $l_{\widetilde{C}\widetilde{D}}^s(0)$ and $L_{\widetilde{C}\widetilde{D}}^s(0)$. If $l_{\widetilde{C}\widetilde{D}}^s(0)$ is larger than $L_{\widetilde{C}\widetilde{D}}^s(0)$, the initial guess should be decreased; if $l_{\widetilde{C}\widetilde{D}}^s(0)$ is smaller than $L_{\widetilde{C}\widetilde{D}}^s(0)$, the initial guess should be increased. Results converge such that $|[L_{\widetilde{C}\widetilde{D}}^s(0) - l_{\widetilde{C}\widetilde{D}}^s(0)]/L_{\widetilde{C}\widetilde{D}}^s(0)| < 0.001\%$

2.3.1.2 Arbitrary state

Tension distributions for the arbitrary state can be calculated based on the tension distributions and the tooth distribution angle of the circular pulley found in the reference state. As mentioned before, pulley will rotate step by step and rotation angle of one step should be picked properly for a better computation performance. The rotation angle of one step for the two-pulley system with a square pulley is chosen as p_p/R_2^s. p_p is the pulley pitch, and R_2^s is the radius of the circular pulley. Rotation relationship between the square pulley and the circular pulley can be got from Equation 2.2.44.

$$\frac{\alpha_1^s}{\alpha_2^s} = \frac{R_2^s}{R_1^s} \tag{2.3.6}$$

α_1^s and α_2^s are the rotation angles of the square pulley and the circular pulley. R_1^s is the equivalent radius of the square pulley. α^s is used to represent the arbitrary state. Following the computation process presented in section 2.2.3, an iteration method starting from the free span CD is used to determine the two free-span tensions. The tension $F_0^s(\alpha)$ in the free span CD, the deflection of the first belt tooth $u_{1,1}^s(\alpha)$ meshed with the square pulley, and the deflection of the first belt tooth $u_{2,1}^s(\alpha)$ meshed with the circular pulley are assigned

initial guesses.

$$F_0^s(\alpha) = f_\alpha^s \tag{2.3.7}$$

$$u_{1,1}^s(\alpha) = u_{1,1\_\alpha}^s \tag{2.3.8}$$

$$u_{2,1}^s(\alpha) = u_{2,1\_\alpha}^s \tag{2.3.9}$$

Tension $F_{1,z_1+1}^s(\alpha)$ and tension $F_{2,z_2+1}^s(\alpha)$ are calculated from the belts meshed with the square pulley and the circular pulley respectively. The initial guess of $u_{2,1}^s(\alpha)$ is then changed by comparing $F_{1,z_1+1}^s(\alpha)$ and $F_{2,z_2+1}^s(\alpha)$. Increase the initial guess if $F_{1,z_1+1}^s(\alpha) > F_{2,z_2+1}^s(\alpha)$, and decrease initial guess if $F_{1,z_1+1}^s(\alpha) < F_{2,z_2+1}^s(\alpha)$ until $F_{1,z_1+1}^s(\alpha)$ and $F_{2,z_2+1}^s(\alpha)$ converge such that $|[F_{1,z_1+1}^s(\alpha) - F_{2,z_2+1}^s(\alpha)]/F_{1,z_1+1}^s(\alpha)| < 0.1\%$.

On the basis of $u_{2,1}^s(\alpha)$ determined in the previous step and the initial guesses of $u_{1,1}^s(\alpha)$ and $F_0^s(\alpha)$, the stretched length ($l_{\widetilde{C}\widetilde{D}}^s(\alpha)$ and $L_{\widetilde{C}\widetilde{D}}^s(\alpha)$) of the span $\widetilde{C}\widetilde{D}(\alpha)$ are calculated for the arbitrary state. If $L_{\widetilde{C}\widetilde{D}}^s(\alpha) > l_{\widetilde{C}\widetilde{D}}^s(\alpha)$, the initial guess of $u_{1,1}^s(\alpha)$ should be increased; if $L_{\widetilde{C}\widetilde{D}}^s(\alpha) < l_{\widetilde{C}\widetilde{D}}^s(\alpha)$, the initial guess of $u_{1,1}(\alpha)$ should be decreased. Results converge such that $|[L_{\widetilde{C}\widetilde{D}}^s(\alpha) - l_{\widetilde{C}\widetilde{D}}^s(\alpha)]/L_{\widetilde{C}\widetilde{D}}(\alpha)| < 0.001\%$.

On the basis of $u_{1,1}^s(\alpha)$ and $u_{2,1}^s(\alpha)$ determined in the previous iteration step and the initial guess of $F_0(\alpha)$, the stretched length ($l_b^s(\alpha)$ and $L_b^s(\alpha)$) of the total pitch line are calculated for the arbitrary state. If $l_b^s(\alpha) > L_b^s(\alpha)$, the initial guess of $F_0(\alpha)$ should be increased; if $l_b^s(\alpha) < L_b^s(\alpha)$, the initial guess of $F_0(\alpha)$ should be decreased. Results converge such that $|[l_b^s(\alpha) - L_b^s(\alpha)]/l_b^s(\alpha)| < 0.001\%$.

Finally, $F_0(\alpha)$ and $F_{n+1}(\alpha)$ are both determined and Equation 2.2.55 can be used to calculate the torque around the circular pulley generated by the square pulley at any state.

2.3.2 Three-pulley system with two oval pulleys

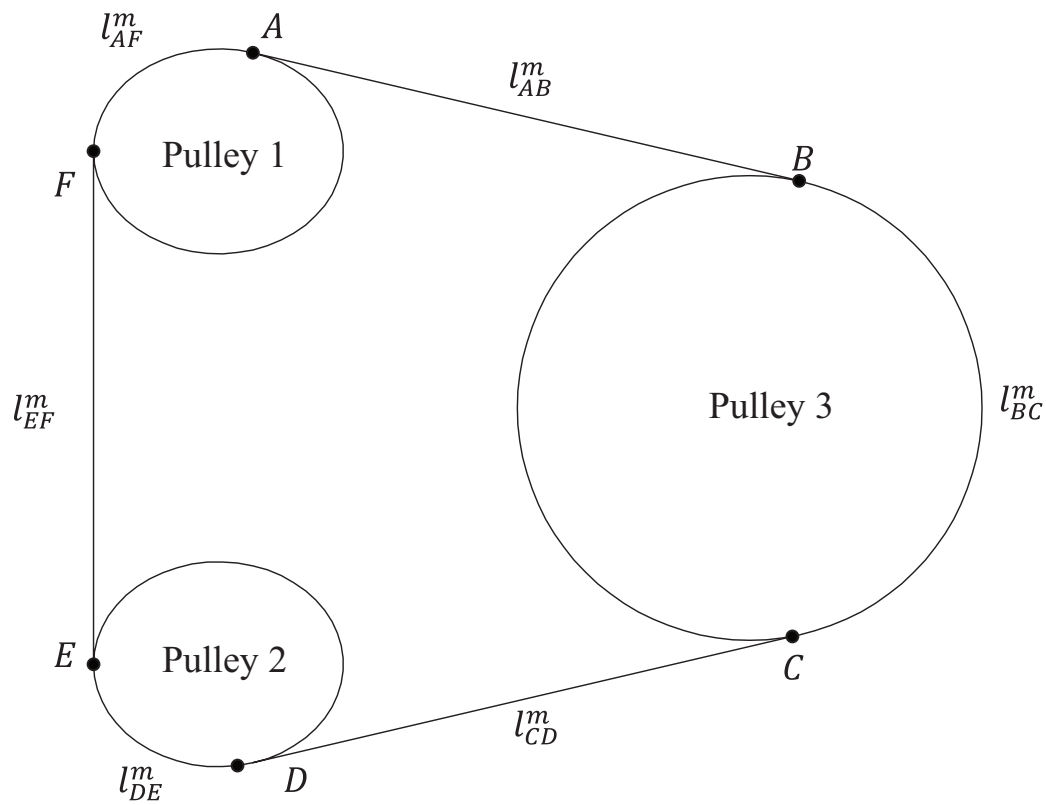

Figure 2.20: Pitch profile of the three-pulley system with two oval pulleys

As already mentioned, two-pulley system is the simplest timing belt system. Multiple pulleys are often used to improve the performance of timing belt drives. Therefore, the multi-pulley system is indispensable. In this section, another oval pulley is added and a three-pulley system with two oval pulleys is built. As shown in Figure 2.20, pulley 1 and pulley 2 are oval pulleys, and pulley 3 is a circular pulley. A, B, C, D, E, and F are tangent points. Stretched lengths of AB, BC, CD, DE, EF, and AF are represented by l_{AB}^m, l_{BC}^m, l_{CD}^m, l_{DE}^m, l_{EF}^m, and l_{AF}^m. The superscript m represents that the value belongs to the multi-pulley system. Pulley teeth and belt teeth in this system are indexed as indicated in Figure 2.21. m_1, m_2, and m_3 are tooth numbers in spans $\widetilde{A}\widetilde{F}$, $\widetilde{B}\widetilde{C}$, and $\widetilde{D}\widetilde{E}$. m_4, m_5, and m_6 introduced later are the belt pitch numbers included in the spans $\widetilde{E}\widetilde{F}$, $\widetilde{C}\widetilde{D}$, and $\widetilde{A}\widetilde{B}$. F_{AB}^m, F_{CD}^m, and F_{EF}^m represent the tensions in the free spans AB, CD, and EF.

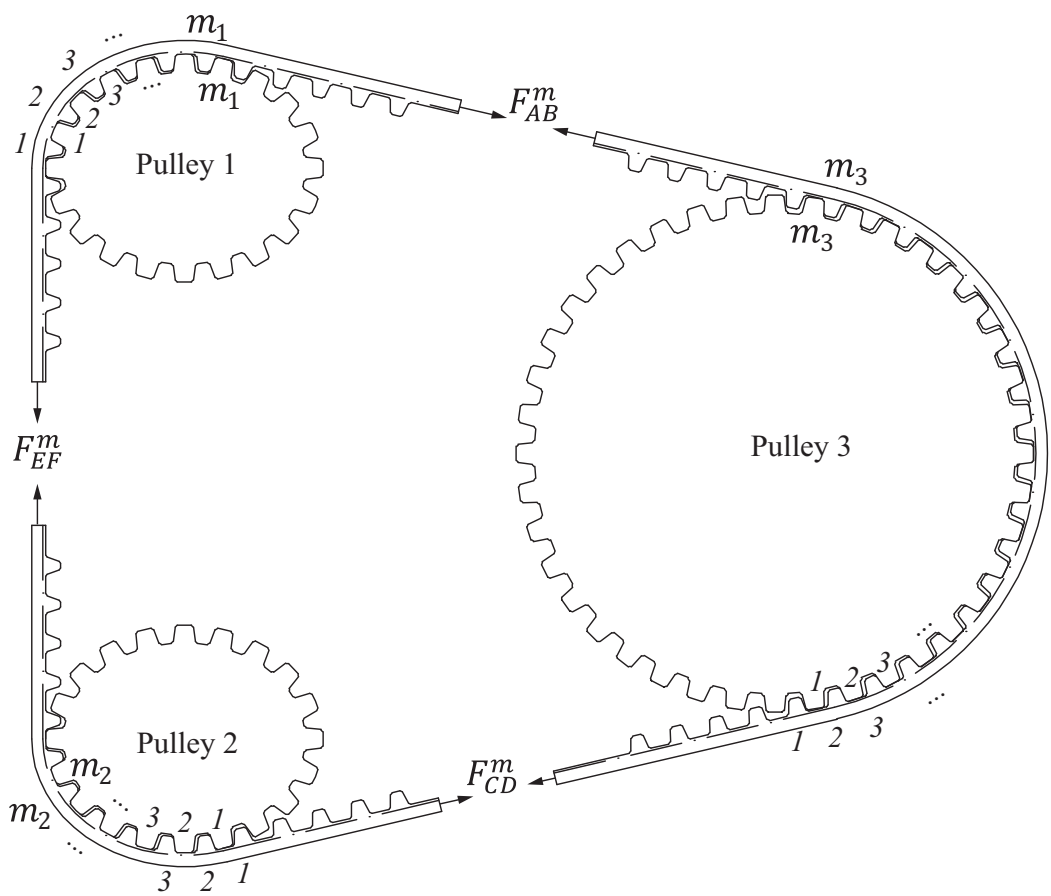

Figure 2.21: Teeth indexes of the three-pulley system with two oval pulleys

Compared to the two-pulley system, the three-pulley system has a new free span and the tension in new free span becomes the third unknown value. As a result, three compatibility conditions are needed. The stretched length of the span $\widetilde{E}\widetilde{F}$ is then used to handle the new unknown tension

$$L^m_{\widetilde{E}\widetilde{F}} = l^m_{\widetilde{E}\widetilde{F}} \tag{2.3.10}$$

$L^m_{\widetilde{E}\widetilde{F}}$ and $l^m_{\widetilde{E}\widetilde{F}}$ can be calculated in a similar way as $L_{\widetilde{C}\widetilde{D}}$ and $l_{\widetilde{C}\widetilde{D}}$ introduced in Section 2.2.1.

2.3.2.1 Reference state

For the reference state, the problem is to determine the values of the free-span tensions and tooth distribution angles of the pulley 1 (top-side oval pulley) and the pulley 3 (right-side circular pulley). Orientation angles of three pulleys and the tooth distribution angle of the pulley 2 (bottom-side oval pulley) are assumed to be zero. Tensions in three free spans are required to be equal. An iteration method starting from the free span CD is used. The general idea of this iteration method has no difference with the previous iteration methods, but a more complex process needs to be considered. A flow chart is established as below.

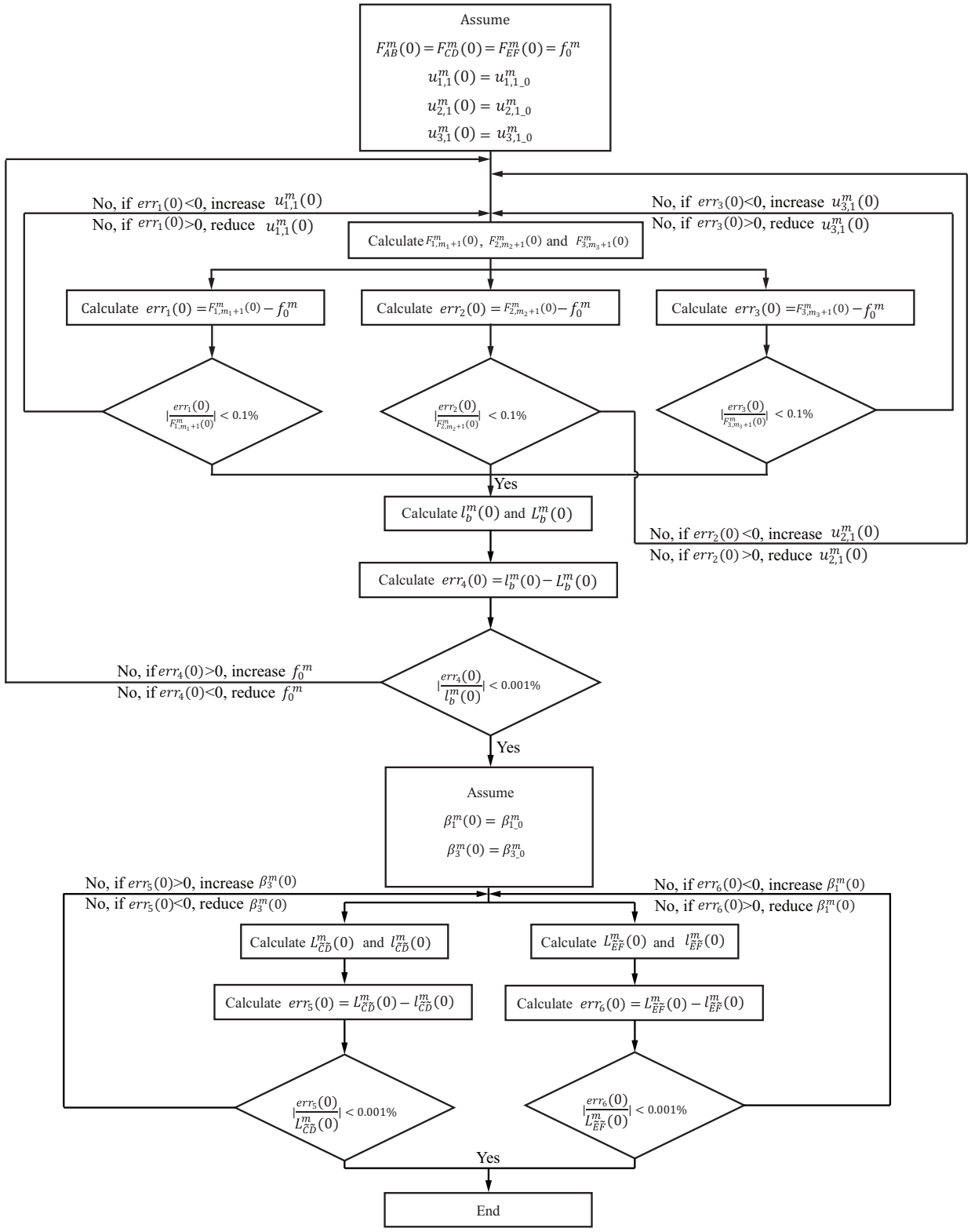

Figure 2.22: Computation process of the belt tension distributions for the three-pulley system in the reference state

The iteration method involves two big iteration loops. The first one is to find the value of the equal free-span tension, which includes three small iteration loops to determine the deflections of the first belt teeth meshed with three pulleys. The second one is to find the tooth distribution angles of pulley 1 and pulley 3 based on the tension distributions determined in the first big iteration loop.

For the first big iteration loop, the value of the equal free-span tension and the deflections of the first belt teeth meshed with three pulleys are assigned initial guesses

$$F_{AB}^{m}(0) = F_{CD}^{m}(0) = F_{EF}^{m}(0) = f_0^m \tag{2.3.11}$$

$$u_{1,1}^{m}(0) = u_{1,1\_0}^{m} \tag{2.3.12}$$

$$u_{2,1}^{m}(0) = u_{2,1\_0}^{m} \tag{2.3.13}$$

$$u_{3,1}^{m}(0) = u_{3,1\_0}^{m} \tag{2.3.14}$$

The previous deflection of the belt tooth, deflection of belt pitch mid-point, and belt tension are assumed to be zero. Tooth load $Q_{2,1}^{m}(0)$, belt tension $F_{2,1}^{m}(0)$, friction force $R_{2,1}^{m}(0)$, and the deflection of the belt pitch mid-point $v_{2,1}^{m}(0)$ are calculated in a similar way to the corresponding values calculated in the reference state for the two-pulley system with an oval pulley. The deflection of the second belt tooth meshed with the pulley 2 can then be calculated relying on the initial guess of $u_{2,1}^{m}(0)$. The tension $F_{2,m_2+1}^{m}(0)$ in the free span EF can be calculated through repeated process from the belts meshed with the pulley 2. $F_{1,m_1+1}^{m}(0)$ and $F_{3,m_3+1}^{m}(0)$ can be got in the same way by $u_{1,1\_0}^{m}$ and $u_{3,1\_0}^{m}$. Compare $F_{1,m_1+1}^{m}(0)$, $F_{2,m_2+1}^{m}(0)$, and $F_{3,m_3+1}^{m}(0)$ with f_0^m to adjust the values of $u_{1,1\_0}^{m}$, $u_{2,1\_0}^{m}$, and $u_{3,1\_0}^{m}$. If $F_{j,m_j+1}^{m}(0) < f_0^m$, $u_{j,1\_0}^{m}$ should be increased; if $F_{j,m_j+1}^{m}(0) > f_0^m$, $u_{j,1\_0}^{m}$ should be decreased. Results converge such that $|[F_{j,m_j+1}^{m}(0) - f_0^m]/f_0^m| < 0.1\%$.

The compatibility condition 2.2.25 is used to find the true value of equal tension in the free spans. $l_b^m(0)$ can be calculated geometrically by the coordinates of tangent points A, B, C, D, E, F, which can be solved similarly using Equation 2.2.10. $L_b^m(0)$ can be calculated using

Equation 2.2.20. Physically, if $l_b^m(0) > L_b^m(0)$, the assumed f_0^m is smaller than the true free-span tension and should be increased in the next iteration step; if $l_b^m(0) < L_b^m(0)$, the assumed f_0^m is larger than the true free-span tension and should be decreased in the next iteration step. In this study, $l_b^m(0)$ and $L_b^m(0)$ converge when $|[l_b^m(0) - L_b^m(0)]/l_b^m(0)| < 0.001\%$.

For the second big iteration loop, tooth distribution angles of the pulley 1 and the pulley 3 are assigned initial guesses

$$\beta_1^m = \beta_{1\_0}^m \tag{2.3.15}$$

$$\beta_3^m = \beta_{3\_0}^m \tag{2.3.16}$$

Stretched lengths of spans $\widetilde{C}\widetilde{D}$ and $\widetilde{E}\widetilde{F}$ can be calculated based on the initial guesses of tooth distribution angles and tension distributions determined by the first big iteration loop.

$$l_{\widetilde{C}\widetilde{D}}^m(0) = l_{CD}^m(0) + d_C^m(0) + d_D^m(0) - 2d_w + u_{2,1}^m(0) + u_{3,1}^m(0) \tag{2.3.17}$$

$$l_{\widetilde{E}\widetilde{F}}^m(0) = l_{EF}^m(0) + d_E^m(0) + d_F^m(0) + u_{1,1}^m(0) - u_{2,m_2}^m(0) \tag{2.3.18}$$

The stretched length of the span $\widetilde{C}\widetilde{D}$ can also be calculated by

$$L_{\widetilde{C}\widetilde{D}}^m(0) = m_5(0)p_b\left[1 + \frac{F_{\widetilde{C}\widetilde{D}}^m(0)}{EA}\right] \tag{2.3.19}$$

$$L_{\widetilde{E}\widetilde{F}}^m(0) = [m_4(0) - 1]p_b\left[1 + \frac{F_{\widetilde{E}\widetilde{F}}^m(0)}{EA}\right] + p_{2,m_2}^m(0) \tag{2.3.20}$$

β_1^m can be determined by making a comparison between $l_{\widetilde{E}\widetilde{F}}^m(0)$ and $L_{\widetilde{E}\widetilde{F}}^m(0)$. If $l_{\widetilde{E}\widetilde{F}}^m(0)$ is larger than $L_{\widetilde{E}\widetilde{F}}^m(0)$, $\beta_{1\_0}^m$ should be decreased in the next iteration step; if $l_{\widetilde{E}\widetilde{F}}^m(0)$ is smaller than $L_{\widetilde{E}\widetilde{F}}^m(0)$, $\beta_{1\_0}^m$ should be increased in the next iteration step. Results converge at $|[L_{\widetilde{E}\widetilde{F}}^m(0) - l_{\widetilde{E}\widetilde{F}}^m(0)]/L_{\widetilde{E}\widetilde{F}}^m(0)| < 0.001\%$. β_3^m can be determined similarly by making a comparison between $l_{\widetilde{C}\widetilde{D}}^m(0)$ and $L_{\widetilde{C}\widetilde{D}}^m(0)$. If $l_{\widetilde{C}\widetilde{D}}^m(0)$ is larger than $L_{\widetilde{C}\widetilde{D}}^m(0)$, $\beta_{3\_0}^m$ should be decreased in the next iteration step; if $l_{\widetilde{C}\widetilde{D}}^m(0)$ is smaller than $L_{\widetilde{C}\widetilde{D}}^m(0)$, $\beta_{3\_0}^m$ should be increased in the next iteration step. Results converge at $|[L_{\widetilde{C}\widetilde{D}}^m(0) - l_{\widetilde{C}\widetilde{D}}^m(0)]/L_{\widetilde{C}\widetilde{D}}^m(0)| < 0.001\%$.

2.3.2.2 Arbitrary state

Tensions in three free spans and deflections of the first belt teeth meshed with the three pulleys are the unknown values for the arbitrary state. A modified iteration method is developed to find these values. The tension in the free span CD and the deflections of the first belt teeth meshed with the three pulleys are assigned initial guesses

$$F^m_{\widetilde{C}\widetilde{D}}(\alpha) = f^m_\alpha \tag{2.3.21}$$

$$u^m_{1,1}(\alpha) = u^m_{1,1\_\alpha} \tag{2.3.22}$$

$$u^m_{2,1}(\alpha) = u^m_{2,1\_\alpha} \tag{2.3.23}$$

$$u^m_{3,1}(\alpha) = u^m_{3,1\_\alpha} \tag{2.3.24}$$

In the first iteration loop, tension $F^m_{\widetilde{E}\widetilde{F}}(\alpha)$ in the free span EF is calculated based on the initial guesses of $F^m_{\widetilde{C}\widetilde{D}}(\alpha)$ and $u^m_{2,1}(\alpha)$. The method is similar to that for the reference state. For the compatibility condition 2.3.10, stretched length of the span $\widetilde{E}\widetilde{F}$ can be calculated by $F^m_{\widetilde{E}\widetilde{F}}(\alpha)$

$$L^m_{\widetilde{E}\widetilde{F}}(\alpha) = [m_4(\alpha) - 1]p_b \left[1 + \frac{F^m_{\widetilde{E}\widetilde{F}}(\alpha)}{EA}\right] + p^m_{2,m_2}(\alpha) \tag{2.3.25}$$

The stretched length of the span $\widetilde{E}\widetilde{F}$ can also be calculated as

$$l^m_{\widetilde{E}\widetilde{F}}(\alpha) = l^m_{EF}(\alpha) + d^m_E(\alpha) + d^m_F(\alpha) + u^m_{1,1}(\alpha) - u^m_{2,m_2}(\alpha) \tag{2.3.26}$$

If $L^m_{\widetilde{E}\widetilde{F}}(\alpha) < l^m_{\widetilde{E}\widetilde{F}}(\alpha)$, $u^m_{1,1}(\alpha)$ should be decreasd, and if $L^m_{\widetilde{E}\widetilde{F}}(\alpha) > l^m_{\widetilde{E}\widetilde{F}}(\alpha)$, $u^m_{1,1}(\alpha)$ should be increased. Results converge at $|[L^m_{\widetilde{E}\widetilde{F}}(\alpha) - l^m_{\widetilde{E}\widetilde{F}}(\alpha)]/L^m_{\widetilde{E}\widetilde{F}}(\alpha)| < 0.001\%$.

In the second iteration loop, tension $F^m_{1,m_1+1}(\alpha)$ in the free span AB is calculated by the tension in the free span EF and $u^m_{1,1}(\alpha)$ determined in the previous iteration loop. Tension $F^m_{3,m_3+1}(\alpha)$ in the free span AB can also be calculated by the initial guesses of $F^m_{\widetilde{C}\widetilde{D}}(\alpha)$ and $u^m_{3,1}(\alpha)$. If $F^m_{1,m_1+1}(\alpha) < F^m_{3,m_3+1}(\alpha)$, $u^m_{3,1\_\alpha}$ should be decreased, and if $F^m_{1,m_1+1}(\alpha) >$

$F^m_{3,m_3+1}(\alpha)$, $u^m_{3,1\_\alpha}$ should be increased. In this study, results converge at $|[F^m_{1,m_1+1}(\alpha) - F^m_{3,m_3+1}(\alpha)]/F^m_{1,m_1+1}(\alpha)| < 0.001\%$.

On the basis of $u^m_{3,1}(\alpha)$ determined from the second iteration loop and the initial guesses of $F^m_{\widetilde{C}\widetilde{D}}(\alpha)$ and $u^m_{2,1}(\alpha)$, compatibility condition 2.2.26 is used to find the value of $u^m_{3,1}(\alpha)$. For the arbitrary state, Equation 2.2.16 gives the first method to calculate the stretched length of the span $\widetilde{C}\widetilde{D}$

$$L^m_{\widetilde{C}\widetilde{D}}(\alpha) = m_5(\alpha)p_b\left[1 + \frac{F^m_{\widetilde{C}\widetilde{D}}(\alpha)}{EA}\right] \tag{2.3.27}$$

Equation 2.2.7 gives the second method to calculate the stretched length of the span $\widetilde{C}\widetilde{D}$

$$l^m_{\widetilde{C}\widetilde{D}}(\alpha) = l^m_{CD}(\alpha) + d^m_C(\alpha) + d^m_D(\alpha) - 2d_w + u^m_{2,1}(\alpha) + u^m_{3,1}(\alpha) \tag{2.3.28}$$

If $L^m_{\widetilde{C}\widetilde{D}}(\alpha)$ is larger than $l^m_{\widetilde{C}\widetilde{D}}(\alpha)$, the value of $u^m_{2,1}(\alpha)$ should be increased; if $L^m_{\widetilde{C}\widetilde{D}}(\alpha)$ is smaller than $l^m_{\widetilde{C}\widetilde{D}}(\alpha)$, the value of $u^m_{2,1}(\alpha)$ should be decreased. Results converge at $|[L^m_{\widetilde{C}\widetilde{D}}(\alpha) - l^m_{\widetilde{C}\widetilde{D}}(\alpha)]/L^m_{\widetilde{C}\widetilde{D}}(\alpha)| < 0.001\%$.

The stretched length of the total pitch line can finally be calculated based on the initial guess of the $F^m_{\widetilde{C}\widetilde{D}}(\alpha)$ and the values ($u^m_{1,1}(\alpha)$, $u^m_{2,1}(\alpha)$, $u^m_{3,1}(\alpha)$) got from the previous computation. Equations 2.2.19 and 2.2.20 give two methods to calculate the stretched length of total pitch line ($l^m_b(\alpha)$ and $L^m_b(\alpha)$). If $l^m_b(\alpha) > L^m_b(\alpha)$, f^m_α is smaller than the true value of $F^m_{\widetilde{C}\widetilde{D}}(\alpha)$ and should be increased; if $l^m_b(\alpha) < L^m_b(\alpha)$, f^m_α is larger than the true value of $F^m_{\widetilde{C}\widetilde{D}}(\alpha)$ and should be decreased. Results converge at $|[l^m_b(\alpha) - L^m_b(\alpha)]/l^m_b(\alpha)| < 0.001\%$.

In the end, true values of $F^m_{\widetilde{C}\widetilde{D}}(\alpha)$, $u^m_{1,1}(\alpha)$, $u^m_{2,1}(\alpha)$ and $u^m_{3,1}(\alpha)$ are determined by the modified iteration method and tensions in other two free spans ($F^m_{\widetilde{A}\widetilde{B}}(\alpha)$ and $F^m_{\widetilde{E}\widetilde{F}}(\alpha)$) are also calculated in the iteration method. Torque around pulley 3 can be calculated as

$$T^m(\alpha) = R^m_3\left[F^m_{\widetilde{C}\widetilde{D}}(\alpha) - F^m_{\widetilde{A}\widetilde{B}}(\alpha)\right] \tag{2.3.29}$$

A flow chart is shown in Figure 2.23 to clarify the solving process.

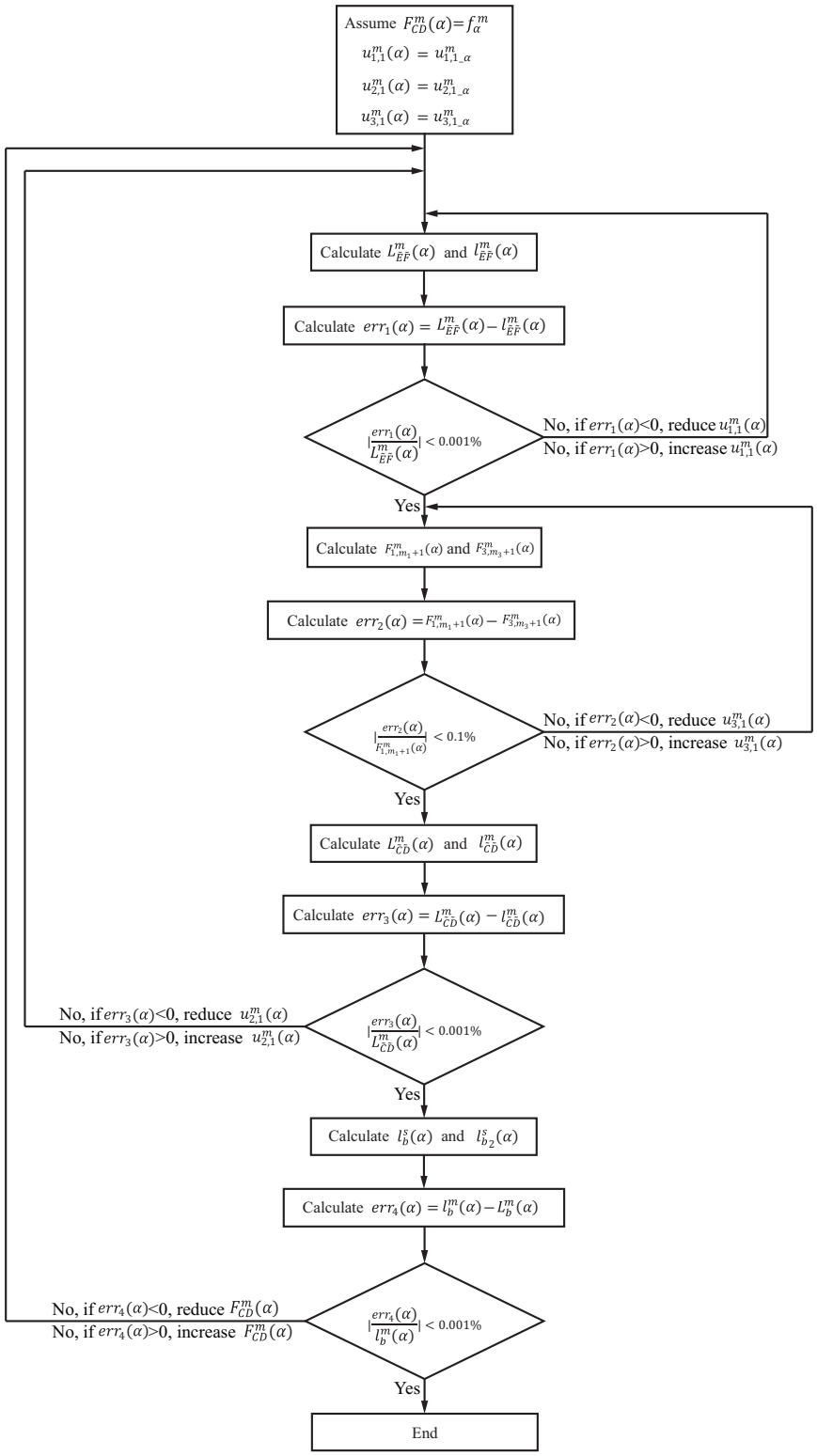

Figure 2.23: Computation process of the belt tension distributions for the three-pulley system in the arbitrary state

2.4 Results

2.4.1 Two-pulley system with an oval pulley

For the two-pulley system with an oval pulley, the data is specified in Table 2.1. O_1O_2 is the center distance between the oval pulley and the circular pulley.

EA (N)	c_R (N/mm)	c_Z (N/mm)	c_G (N/mm)	p_b (mm)	ε (mm)	O_1O_2 (mm)	β_1 (rad)	b (mm)
270000	33750	168.75	80	8	1.5	198.5	0	0.15

Table 2.1: Parameters for the two-pulley system with an oval pulley

The stretched lengths of the free spans AB and CD are shown in Figure 2.24.

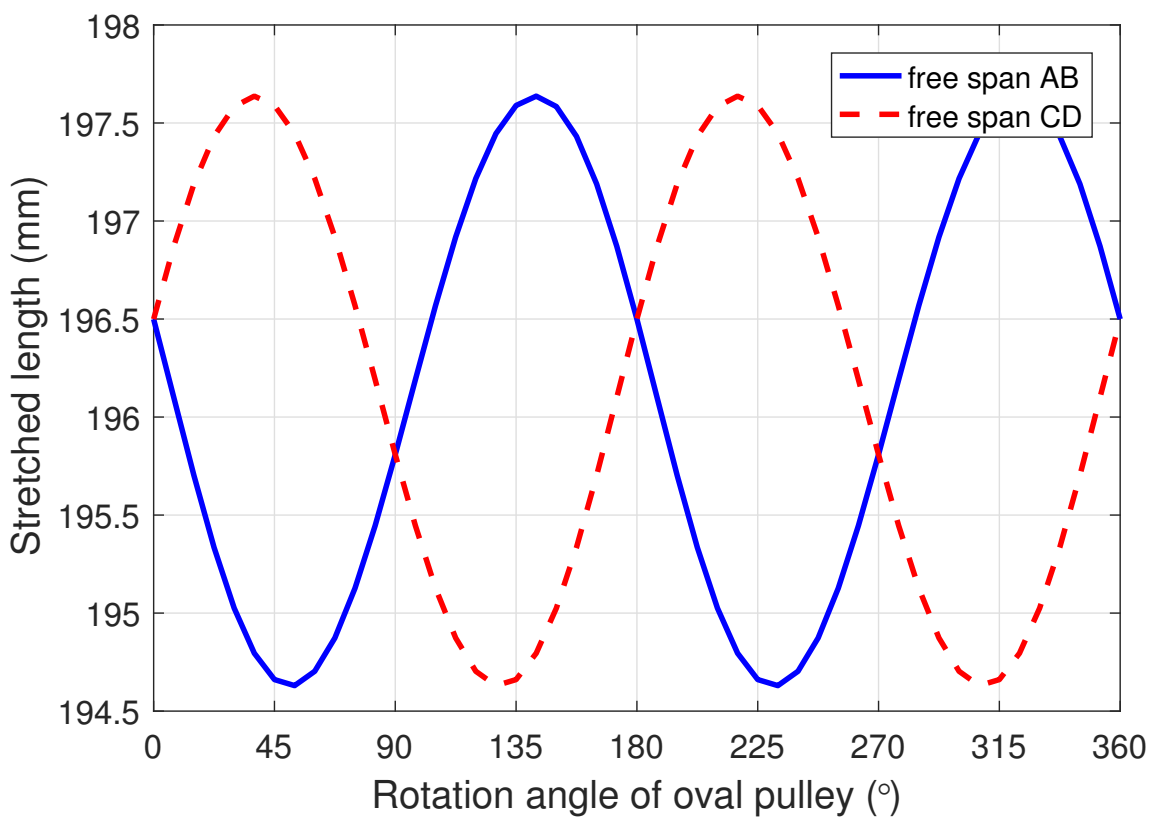

Figure 2.24: Stretched lengths of the free spans AB and CD for the two-pulley system with an oval pulley

When the rotation angle of the oval pulley is equal to $n\pi/2$ ($n = 1, 2, 3...$), the semi-major axis or the semi-minor axis is parallel to the centerline of the two pulleys, and the timing belt system is symmetrical with respect to this centerline. Therefore, the stretched lengths of the free span AB is equal to the stretched length of the free span CD in these conditions. Due to the difference between the lengths of semi-major axis and semi-minor axis, the free-span stretched lengths calculated when the semi-major axis is parallel to the centerline are different from those calculated when the semi-minor axis is parallel to the centerline.

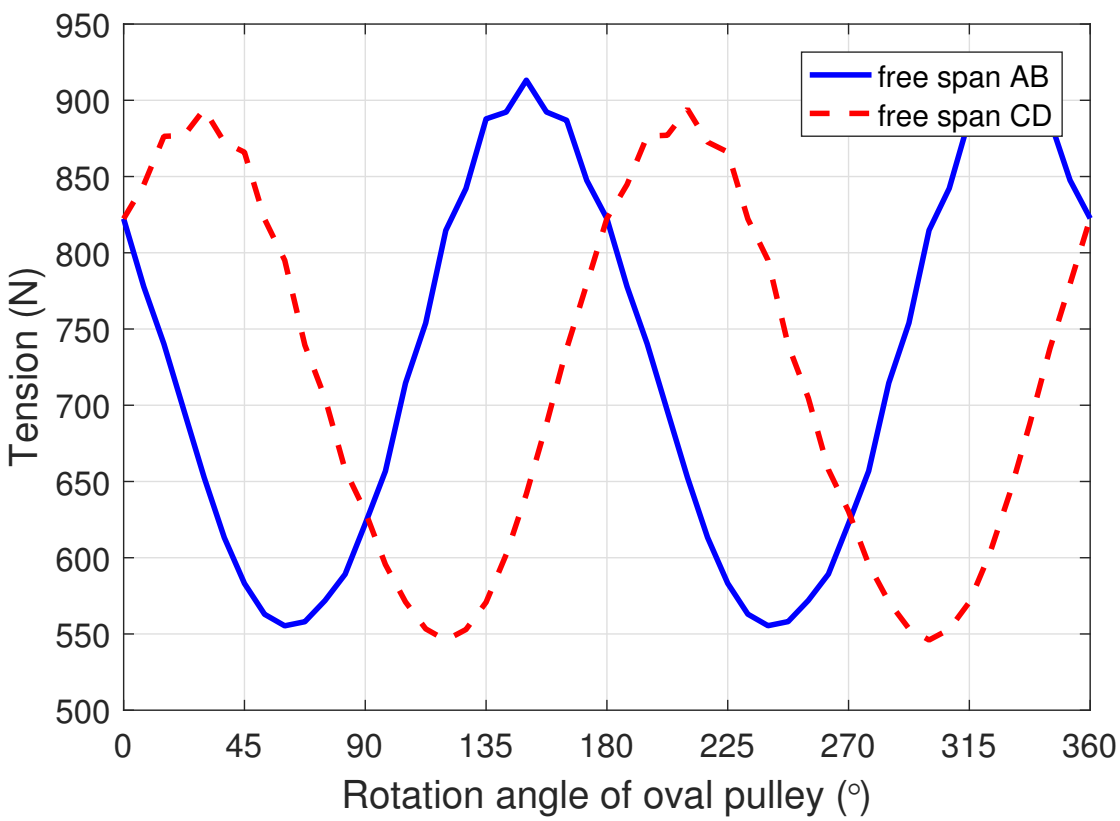

Figure 2.25: Tensions in the free spans AB and CD for the two-pulley system with an oval pulley

Tensions in the free spans AB and CD are shown in Figure 2.25. It is found that the free-span tension changes with the variation of the free-span stretched length. Partial meshing between the belt teeth and the pulley teeth near the tangent points is not considered in this

work. Therefore, when the meshing state of one belt tooth changes, belt tension will go through a steep variation.

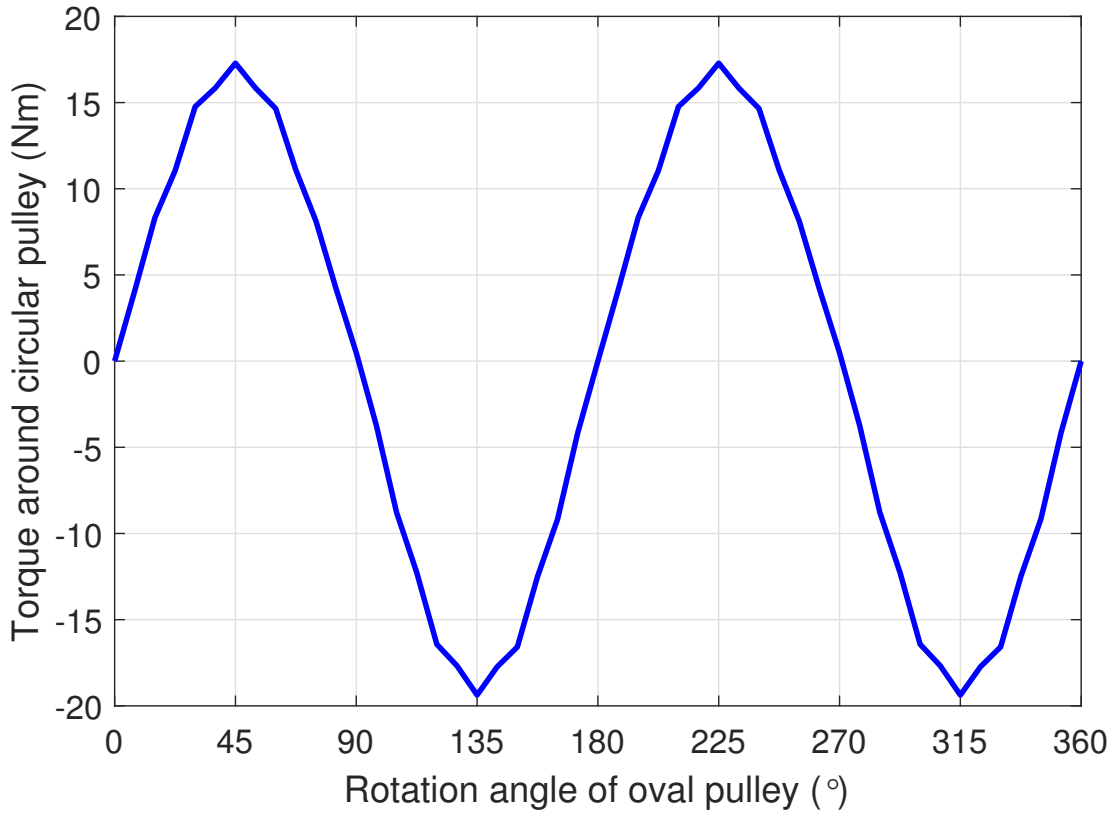

Figure 2.26: Torque around the circular pulley for the two-pulley system with an oval pulley

The corrective torque generated by the rotation of the oval pulley is shown in Figure 2.26. The torque is zero when the system is symmetrical and changes with the difference between the two free-span tensions. As mentioned before, the free-span tensions are related to the stretched lengths of the free spans. When the rotation angle of the oval pulley gets to 45°, the difference between the stretched lengths of the two free spans gets to the positive maximum value, as indicated on the Figure 2.27. Therefore, the torque reaches its positive maximum value when the rotation angle of the oval pulley is 45°. Similarly, when the rotation angle is 135°, the torque reaches its negative maximum value.

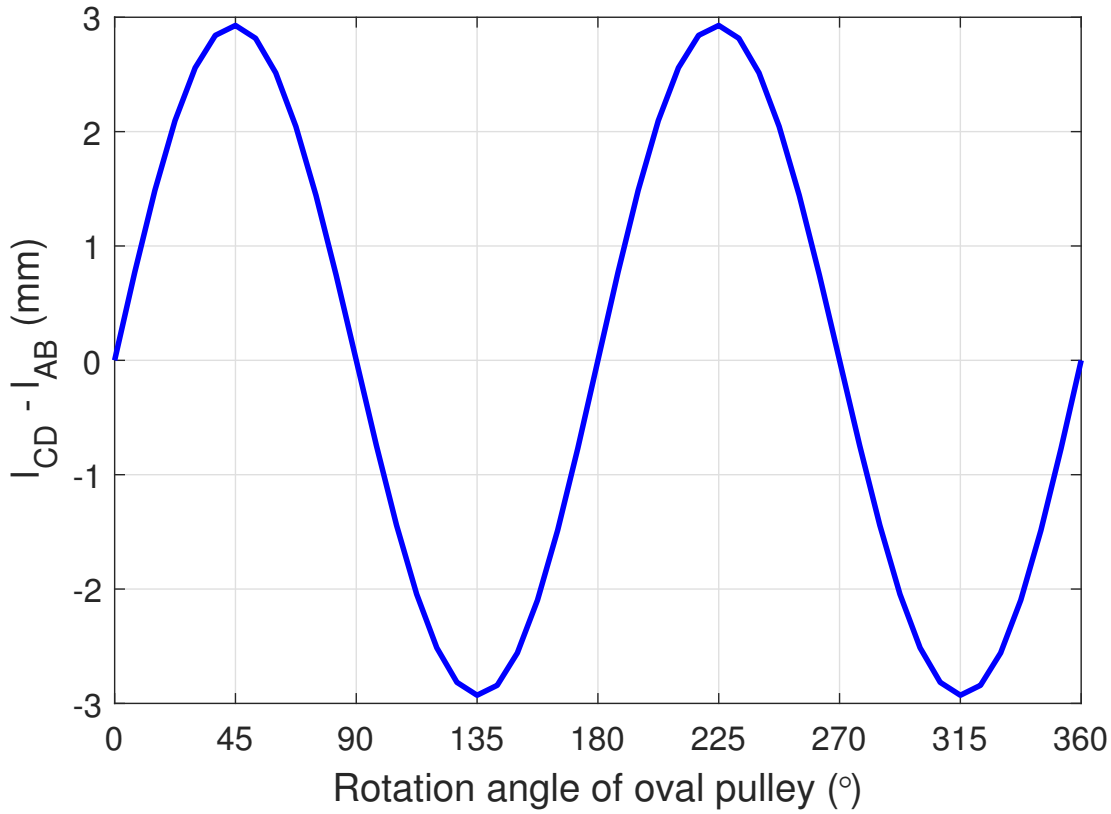

Figure 2.27: The difference between the stretched lengths of the free spans AB and CD for the two-pulley system with an oval pulley

According to the relationship between the torque and the rotation angle of the oval pulley, the phase of the torque can be adjusted by changing the orientation angle of the oval pulley in the reference state. As indicated in the Figure 2.28, the torques start from the positive and negative maximum value with the orientation angles $\gamma_1 = 45°$ and $\gamma_1 = 135°$, respectively. The torque with the orientation angle $\gamma_1 = 90°$ and the torque with the orientation angle $\gamma_1 = 0°$ are out of phase.

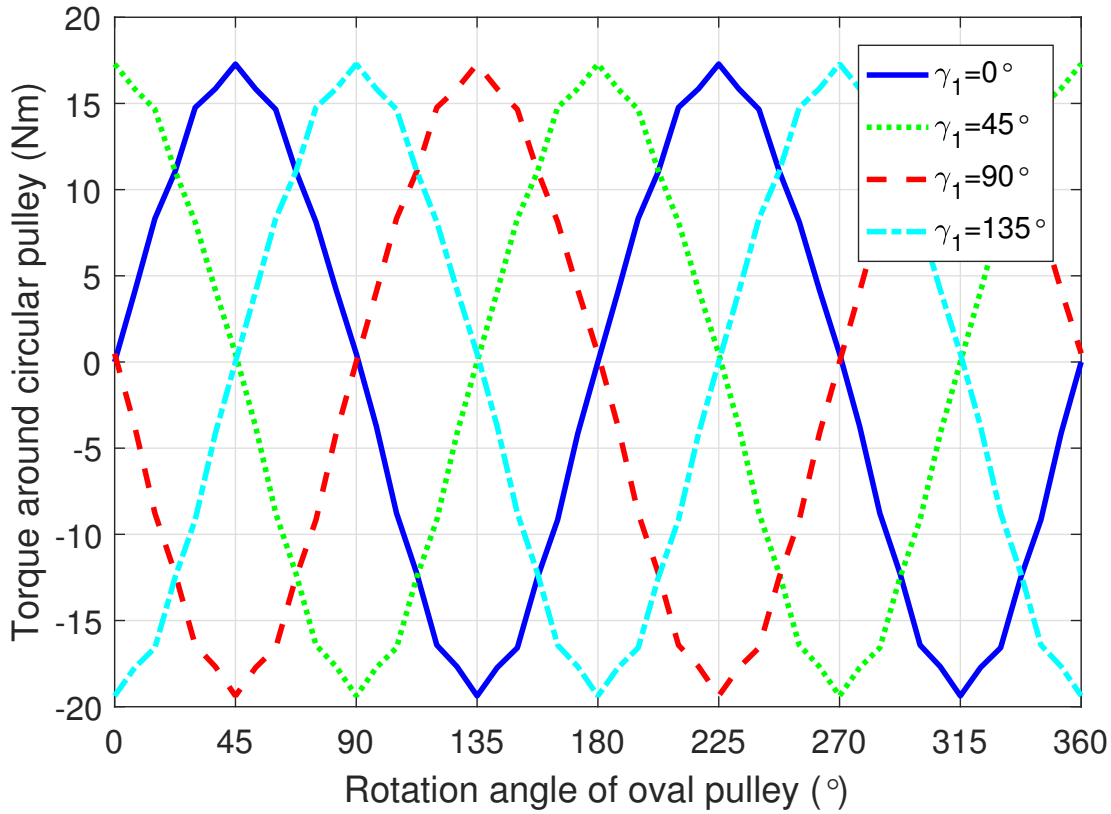

Figure 2.28: The relationship between the phase of the torque and the orientation angle (γ_1) of the oval pulley in the two-pulley system with an oval pulley

The relationship between the diameter difference ε and the torque amplitude is shown in Figure 2.29. All the other values are the same as those specified in Table 2.1. It is found that the amplitude of the torque changes almost linearly with the variation of the difference between the diameters of the oval pulley and its equivalent circular pulley, which is helpful to determine the shape of the oval pulley for a specific torsional vibration.

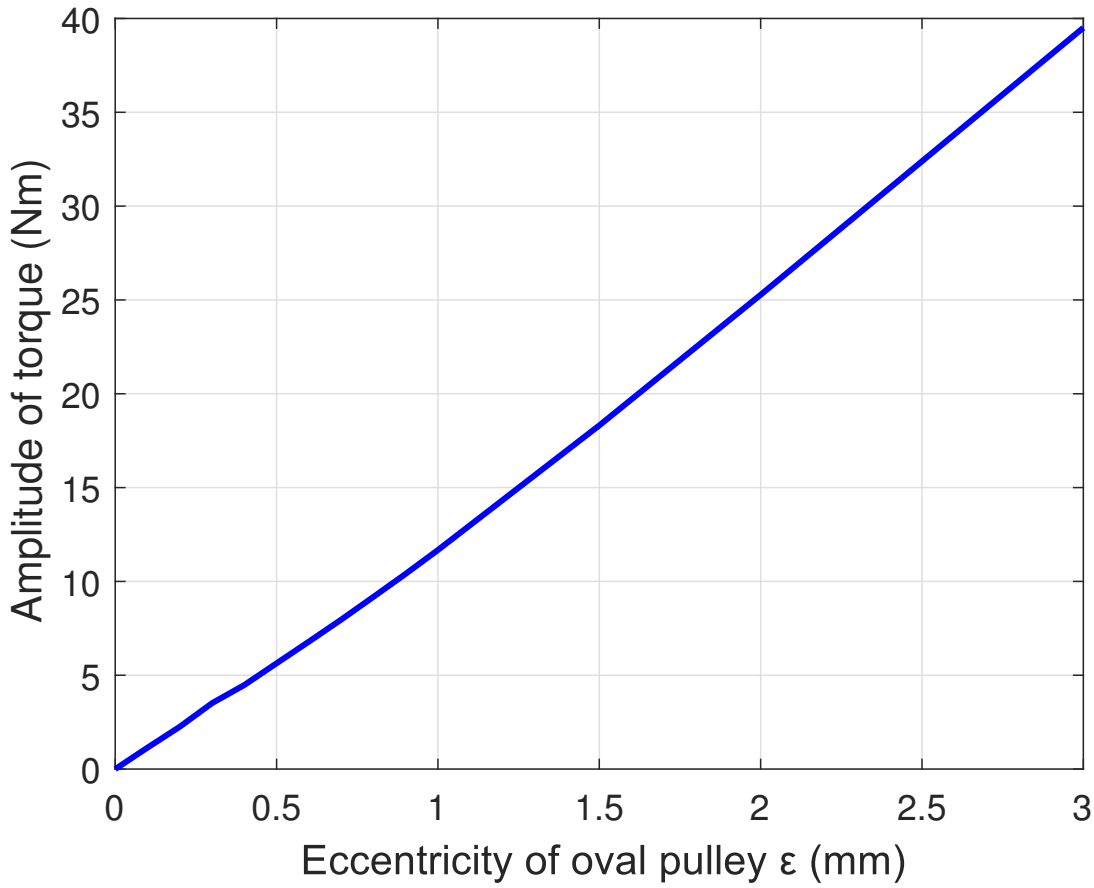

Figure 2.29: The relationship between the eccentricity of the oval pulley (ε) and the amplitude of the corrective torque around the circular pulley in the two-pulley system with an oval pulley

2.4.2 Two-pulley system with an inflated rounded square pulley

For two-pulley system with a square pulley, the data is specified in Table 2.2. O_1O_2 is the center distance between the square pulley and the circular pulley.

EA (N)	c_R (N/mm)	c_Z (N/mm)	c_G (N/mm)	p_b (mm)	ε^s (mm)	O_1O_2 (mm)	β_1 (rad)	b (mm)
270000	33750	168.75	200	8	1.5	203	0	0.15

Table 2.2: Parameters for the two-pulley system with a square pulley

The stretched lengths of the free spans AB and CD are shown in Figure 2.30. For the square-pulley system, similar phenomenon can be found. Free-span tensions change with the variations of the free-span stretched lengths (Figure 2.31). The only difference between the oval-pulley system and the square-pulley system is the radius variation. The period is $\pi/2$ for the square pulley, while the period is π for the oval pulley. Therefore, the period of the torque generated by the square pulley is $\pi/2$ (as indicated in Figure 2.32), which can be used to cancel the special fluctuating torque with the same period. As shown in the Figure 2.34, the torques generated by the square pulley with the orientation angles $\gamma_1^s = 22.5°$ and $\gamma_1^s = 67.5°$ start from the negative and the positive maximum value, respectively. The torques with the orientation angles $\gamma_1 = 0°$ and $\gamma_1 = 45°$ respectively are out of phase. At last, the relationship between the amplitude of the generated torque and the diameter difference ε^s is shown in the Figure 2.35. The amplitude of the torque changes linearly with the variation of the diameter difference between the square pulley and its equivalent circular pulley.

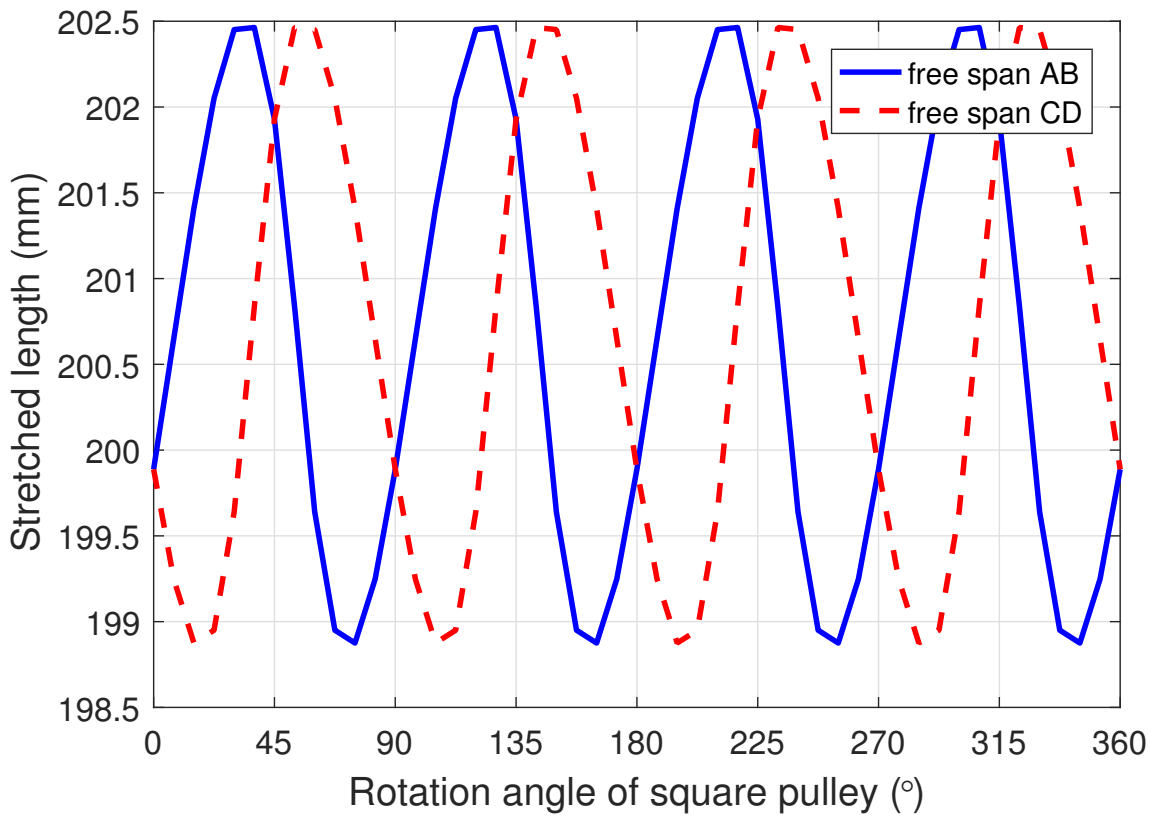

Figure 2.30: Stretched lengths of the free spans AB and CD for the two-pulley system with a square pulley

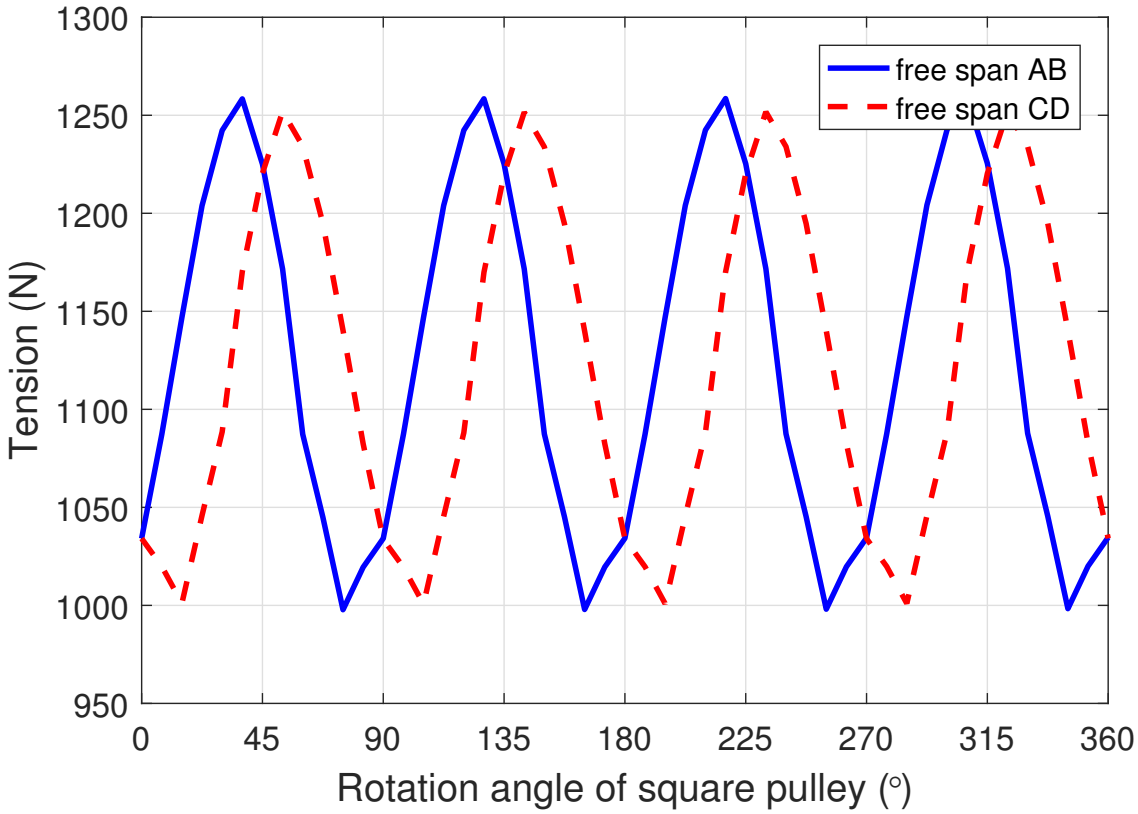

Figure 2.31: Tensions in the free spans AB and CD for the two-pulley system with a square pulley

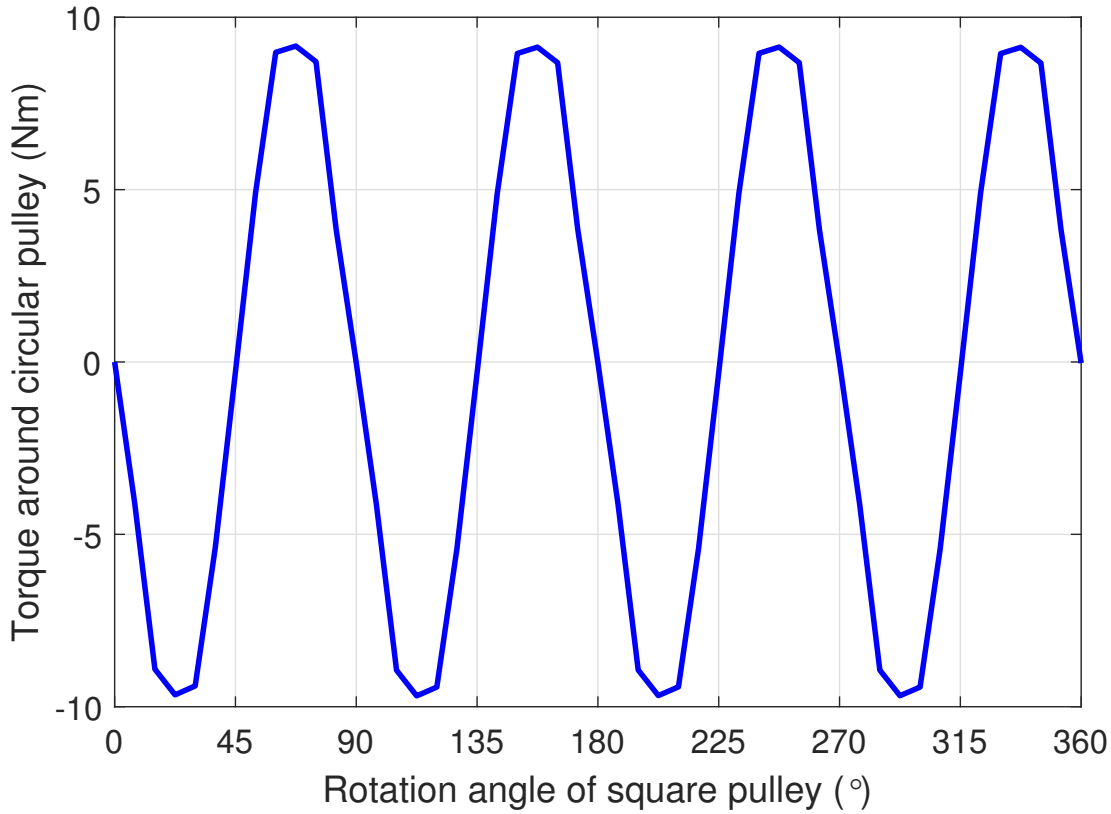

Figure 2.32: Torque around the circular pulley for the two-pulley system with a square pulley

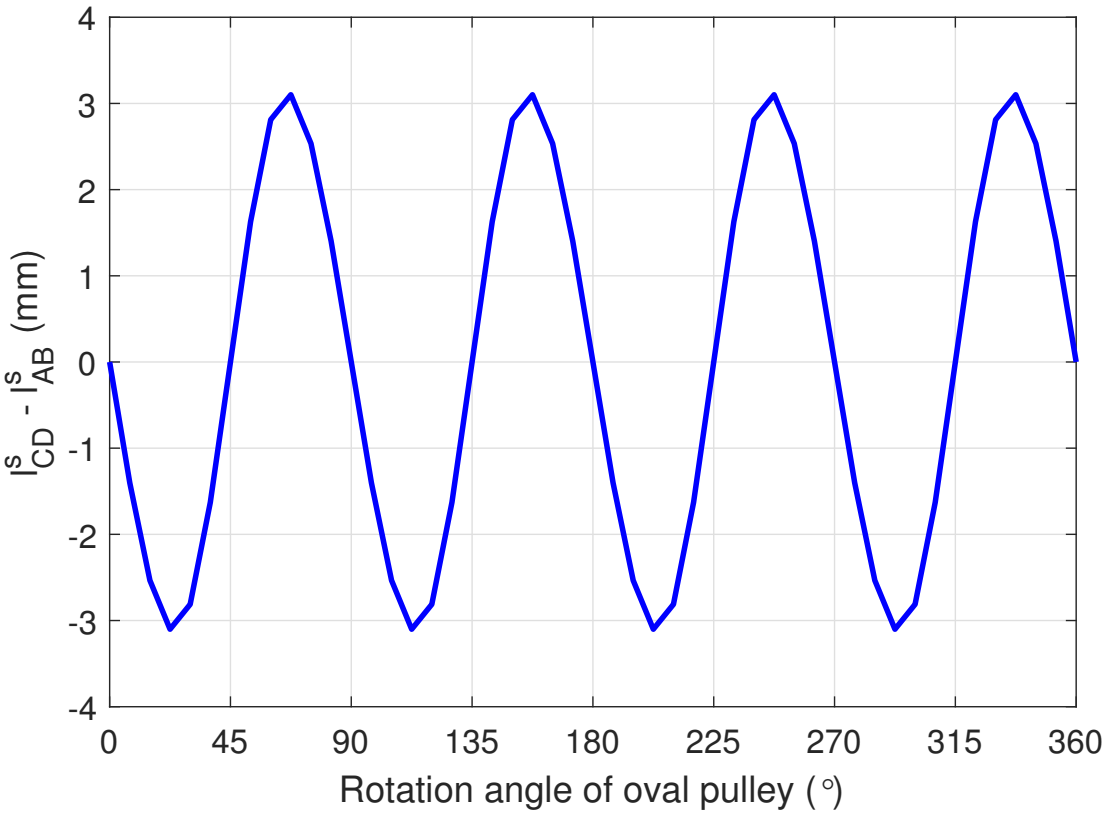

Figure 2.33: The difference between the stretched lengths of the free spans AB and CD for the two-pulley system with a square pulley

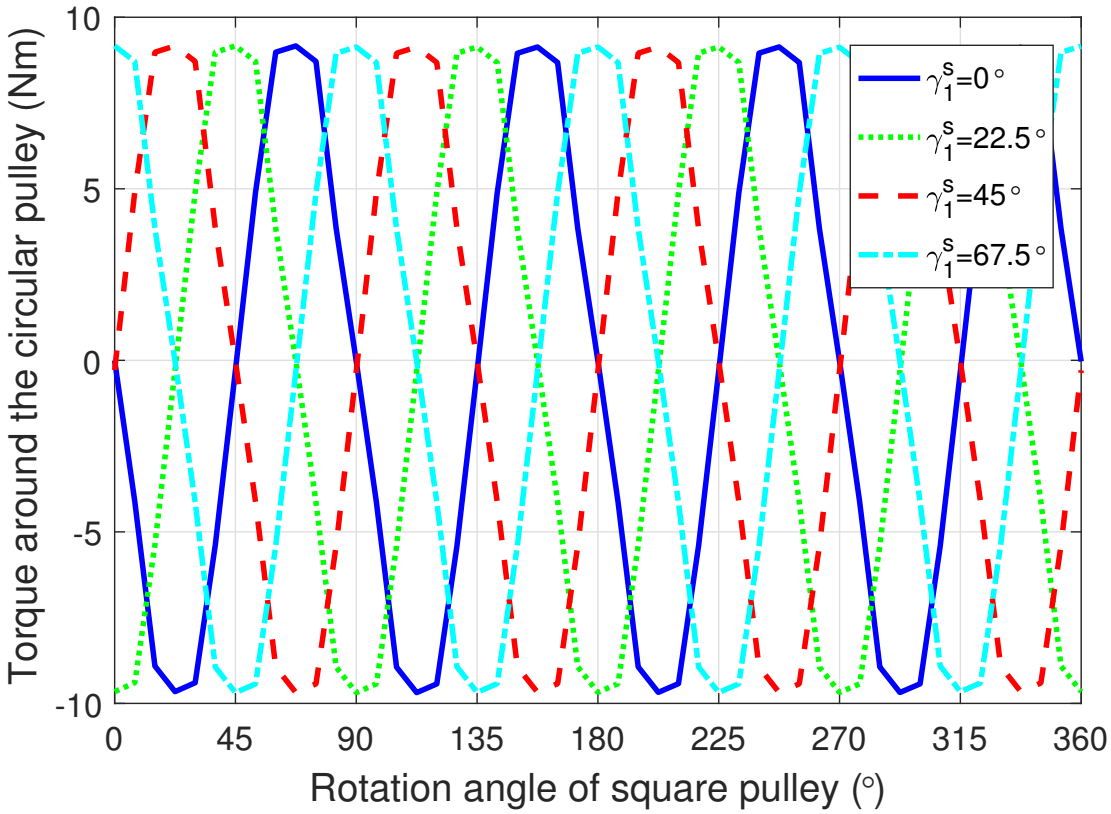

Figure 2.34: The relationship between the phase of the torque and the orientation angle (γ_1^s) of the square pulley in the two-pulley system with a square pulley

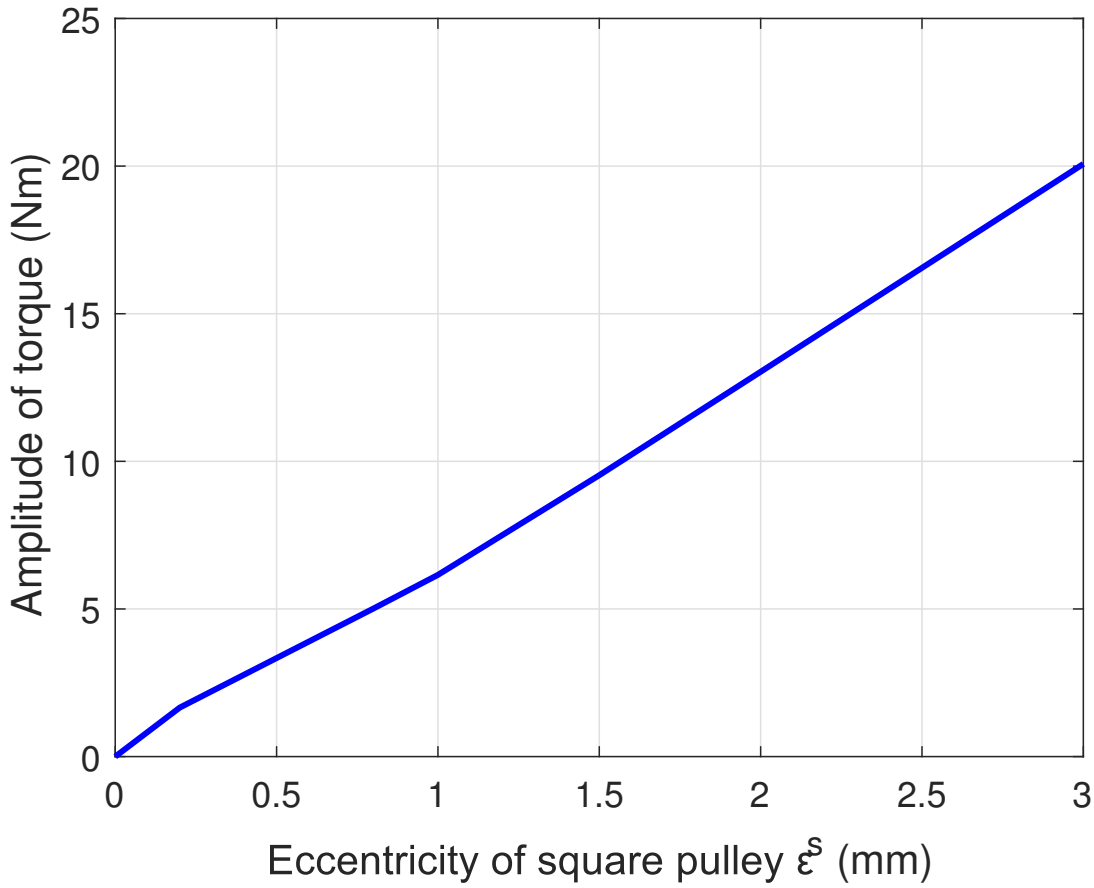

Figure 2.35: The relationship between the eccentricity of the square pulley (ε^s) and the amplitude of the corrective torque around the circular pulley in the two-pulley system with a square pulley

2.4.3 Three-pulley system with two oval pulleys

EA (N)	c_R (N/mm)	c_Z (N/mm)	c_G (N/mm)	p_b (mm)	ε^m (mm)	β_2 (rad)	b (mm)
270000	33750	168.75	350	8	0.92	0	0.15

O_1O_2 (mm)	O_1O_3 (mm)	O_2O_3 (mm)
400	286	286

Table 2.3: Parameters for the three-pulley system with two oval pulleys

For three-pulley system with two oval pulleys, the data is specified in Table 2.3. O_1O_2 is the center distance between pulley 1 and pulley 2. O_2O_3 is the center distance between pulley 2 and pulley 3. O_1O_3 is the center distance between pulley 1 and pulley 3. The stretched lengths of the free spans AB and CD are shown in Figure 2.36. Due to the positions of the pulley 1 and pulley 2, the stretched length of free span EF is a constant (400 mm), and the difference between the stretched length of the free spans AB and CD is relatively smaller than the previous two systems. As a result, the amplitude of the torque generated by this multi-pulley system is small. For the detailed information, the free-span tensions are shown in Figure 2.37. The tension in the free span EF is not included, because only the tensions in the free spans AB and CD are needed to calculate the corrective torque around the circular pulley. The torque is shown in Figure 2.38, which follows the change of the stretched length difference between the free spans AB and CD (Figure 2.39). The relationship between the phase of the torque and the orientation angles of the oval pulleys is shown in Figure 2.40. The relationship between the amplitude of the torque and the diameter difference ε of the oval pulley is shown in Figure 2.41.

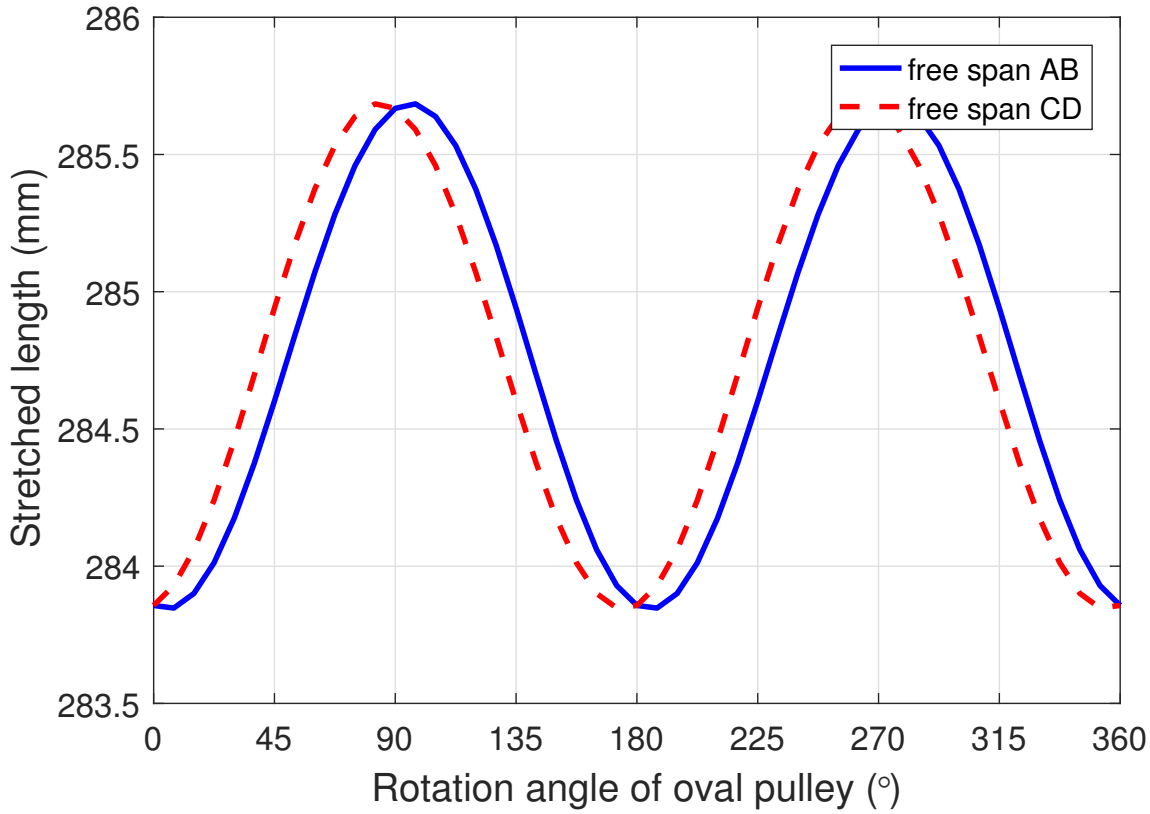

Figure 2.36: Stretched lengths of the free spans AB and CD for the three-pulley system with two oval pulleys

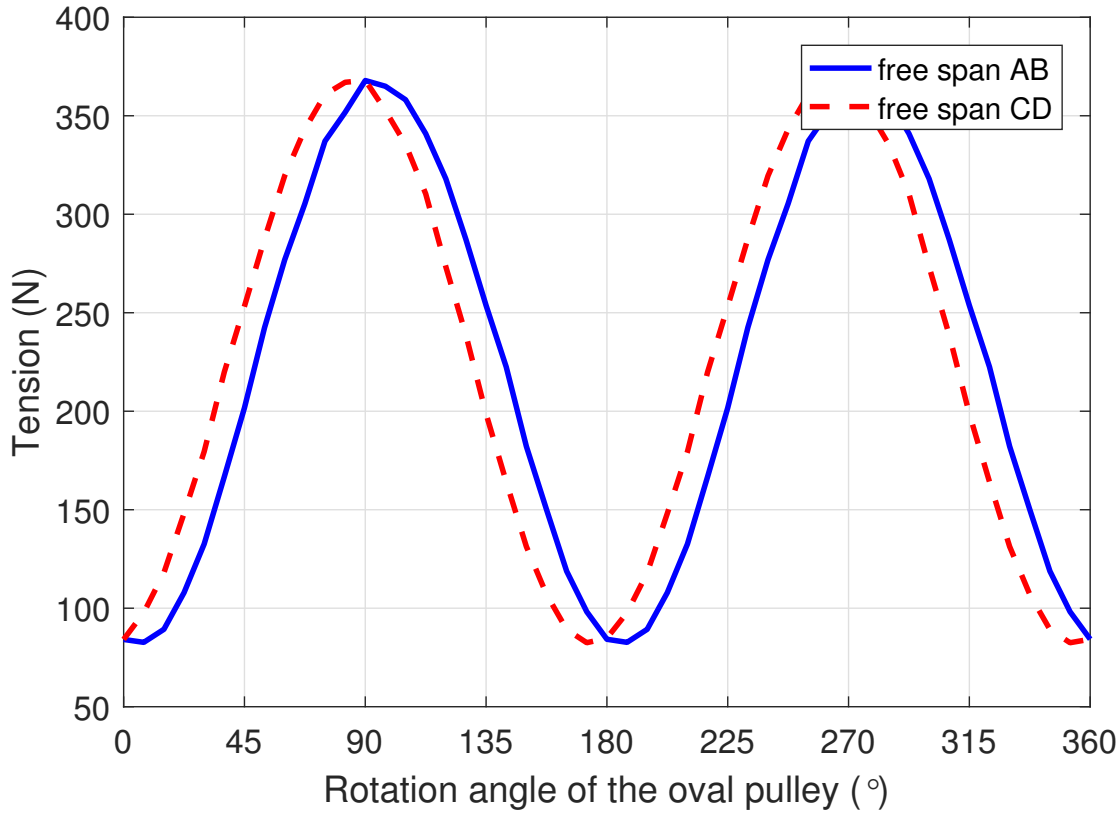

Figure 2.37: Tensions in the free spans AB and CD for the three-pulley system with two oval pulleys

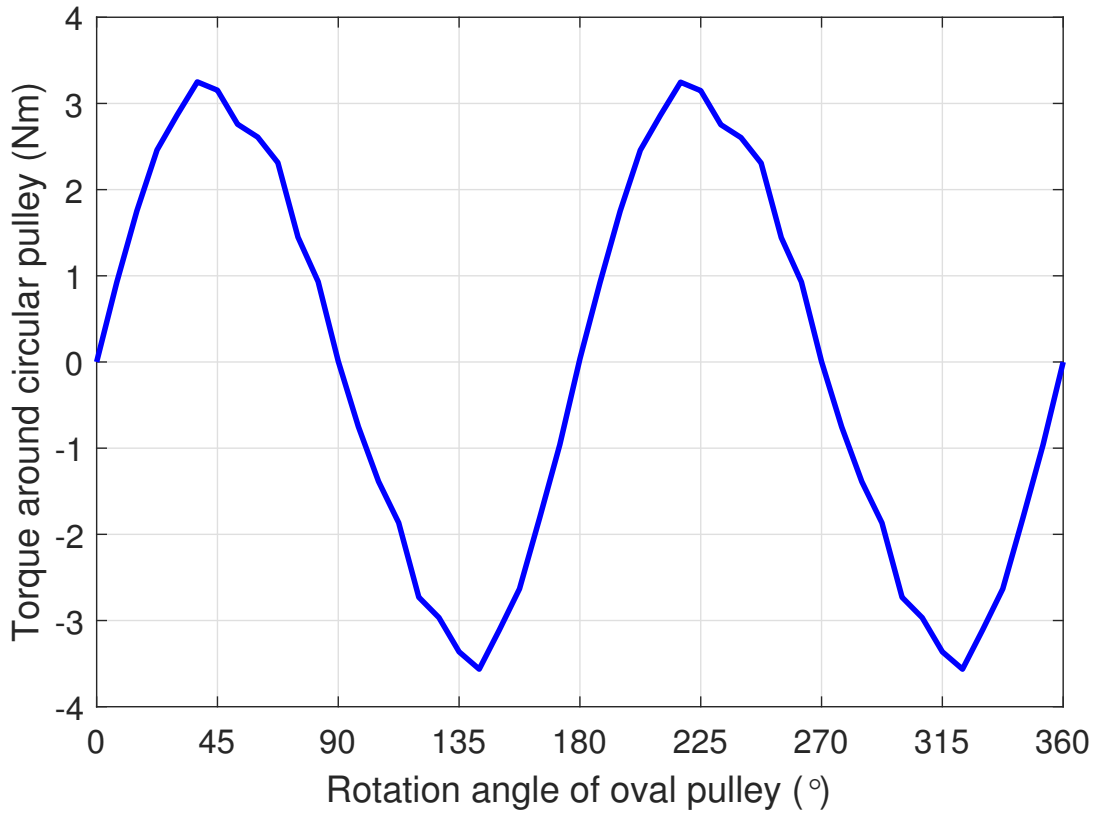

Figure 2.38: Torque around the circular pulley for the three-pulley system with two oval pulleys

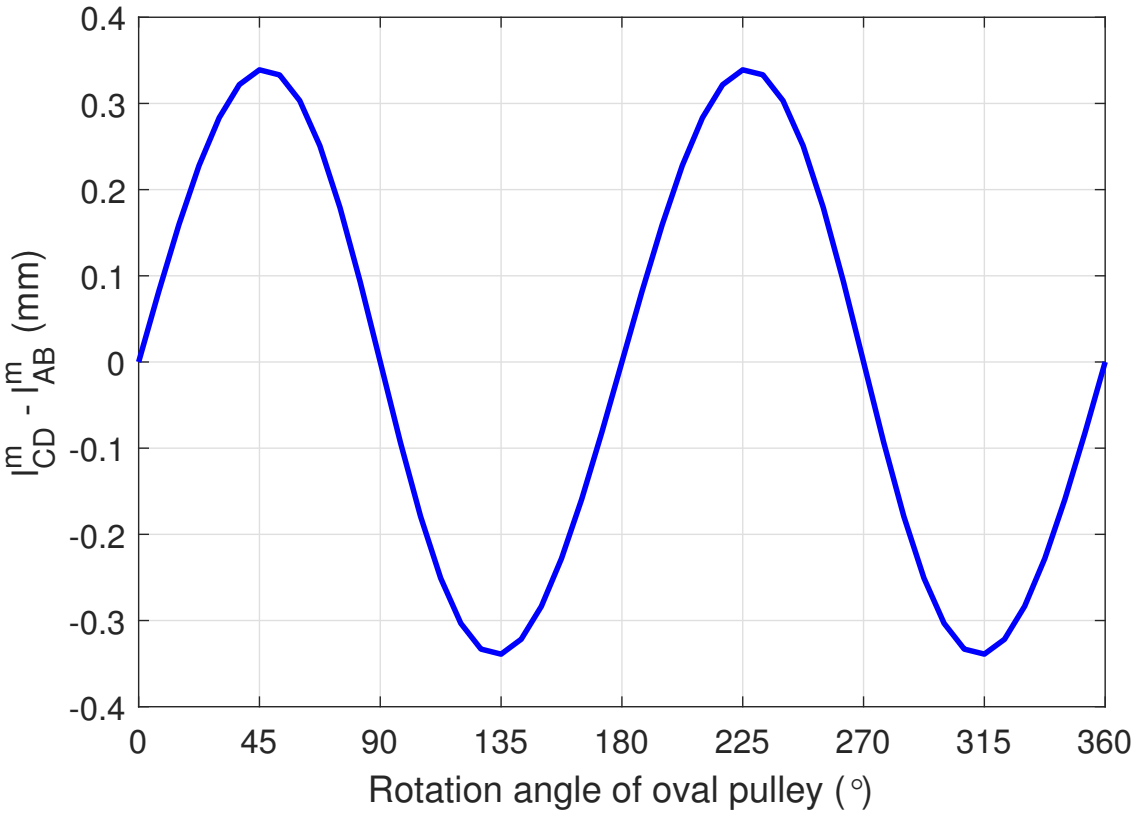

Figure 2.39: The difference between the stretched lengths of the free spans AB and CD for the three-pulley system with two oval pulleys

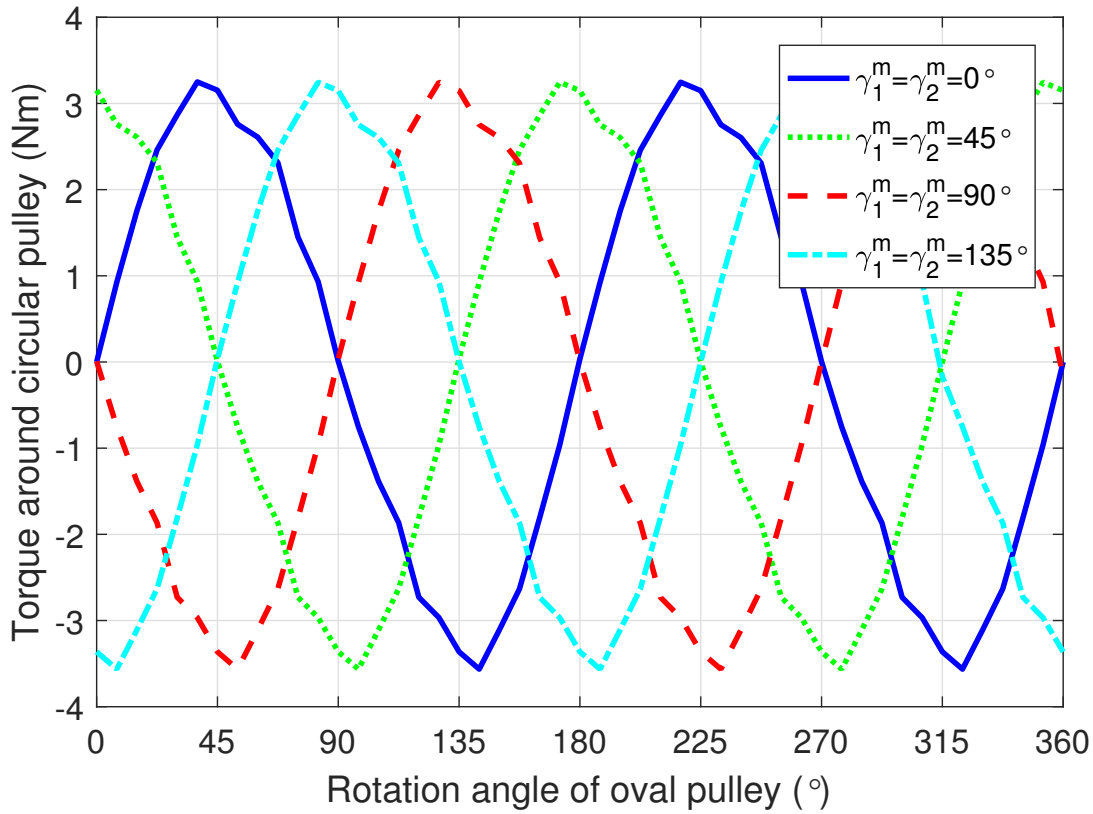

Figure 2.40: The relationship between the phase of the torque and the orientation angles (γ_1^m, γ_2^m) of the oval pulleys in the three-pulley system with two oval pulleys

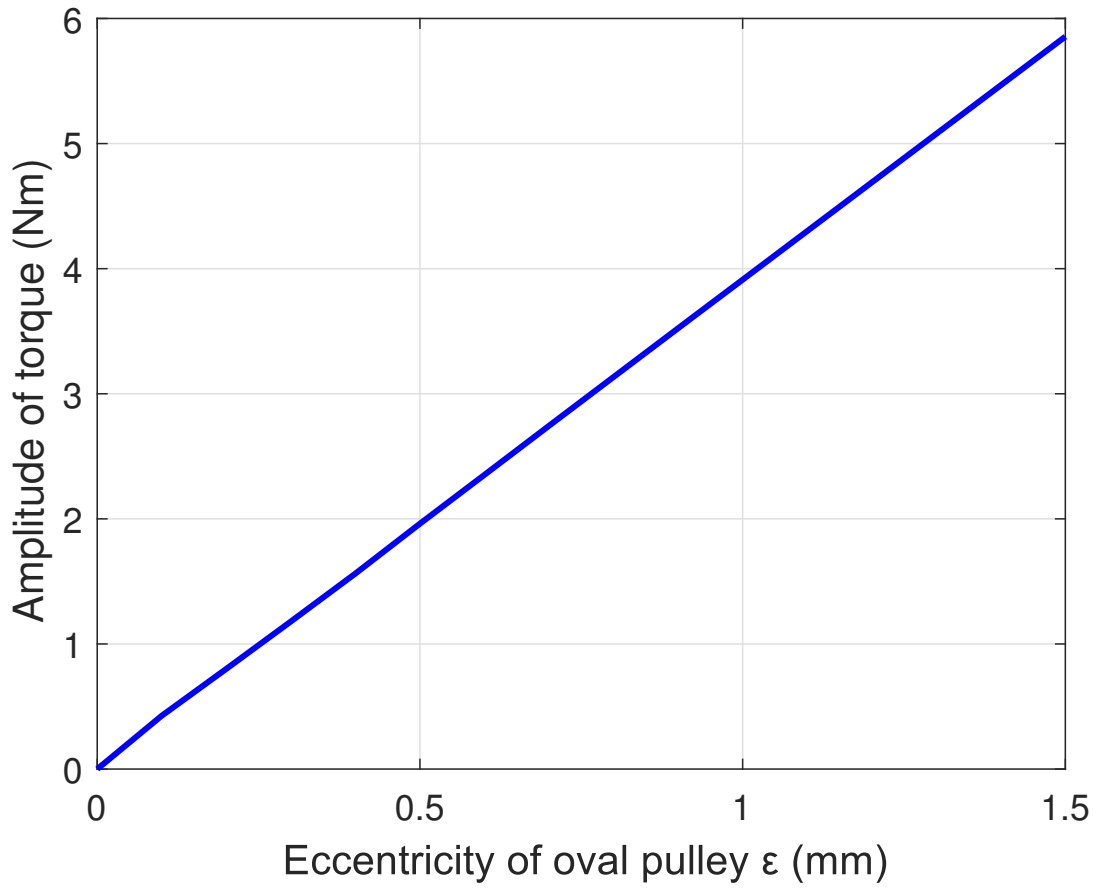

Figure 2.41: The relationship between the eccentricities of the oval pulleys (ε) and the amplitude of the corrective torque around the circular pulley in the three-pulley system with two oval pulleys

Chapter 3

Conclusions

Two compatibility conditions are found to solve the two unknown tensions in the two free spans caused by the replacement of a circular pulley with an oval pulley. A computational model using nested iterative method has been built to determine the distribution angles along the pulley, tension distributions around the belt, deflections of belt teeth, and tooth loads between two meshed teeth. Friction force history is considered in the model to calculate load conditions of the timing belt system at an arbitrary rotation angle of the oval pulley. More complex timing belt systems are analyzed to give a general solution to different timing belt drive systems.

From previously presented results, the following conclusions can be drawn:

1. Replacing circular driving pulley with noncircular driving pulley will lead to periodically changing free-span stretched lengths, which will give rise to a periodically changing torque around pulleys. The periodic torque can be used to cancel undesired torsional vibration. Meanwhile, the form of the torque is related to the geometry of the noncircular pulley. The period of the generated torque is related to the variation of the radius along with the rotation of the noncircular pulley.

2. This model can be used to quickly calculate tooth load for each belt tooth in contact,

friction force between pulley tooth top and belt groove, belt tension distributions, and torque around the circular pulley. It is found that the amplitude of the torque changes linearly with the variation of the diameter difference between the noncircular pulley and its equivalent circular pulley. Meanwhile, this model can be used to study the effect of other easily managed properties, such as the backlash, the stiffness constant, and the tooth distribution angle on the amplitude of the generated torque. This model can also be used to predict load conditions in the reference state when the configuration of the system is specified.

3. This model has introduced a method of combining the spring-based model with the iteration method to calculate the dynamic loadings for different timing belt systems. It can be updated if there is a new model developed for a newly designed type of timing belt.

Bibliography

[1] G Gerbert, H Jonsson, U Persson, and G Stensson. Load distribution in timing belts. *Journal of Mechanical Design*, 100(2):208–215, 1978.

[2] MR Naji and KM Marshek. Toothed belt-load distribution. *Journal of Mechanisms, Transmissions, and Automation in Design*, 105(3):339–347, 1983.

[3] Masanori KAGOTANI, Tomio KOYAMA, Hiroyuki UEDA, Toshio AIDA, and Takeshi HOSHIRO. Load distribution on toothed belt drives under a state of initial tension. *Bulletin of JSME*, 27(230):1780–1787, 1984.

[4] Kazuki Shimizu and Toru Fujii. A simple modeling for analyzing the load distribution of toothed belts under fluctuating torque loading. Technical report, SAE Technical Paper, 1995.

[5] Nestor A Karolev and Peter W Gold. Load distribution of timing belt drives transmitting variable torques. *Mechanism and machine theory*, 30(4):553–567, 1995.

[6] THC Childs, KW Dalgarno, MH Hojjati, MJ Tutt, and Andrew J Day. The meshing of timing belt teeth in pulley grooves. *Proceedings of the Institution of Mechanical Engineers, Part D: Journal of Automobile Engineering*, 211(3):205–218, 1997.

[7] Tomas Johannesson and Martin Distner. Dynamic loading of synchronous belts. *Journal of Mechanical Design*, 124(1):79–85, 2002.

[8] Witold Gajewski. Synchronous drive apparatus and methods, May 16 2006. US Patent 7,044,875.

[9] XF Wang and WD Zhu. Dynamic analysis of an automotive belt-drive system with a noncircular sprocket by a modified incremental harmonic balance method. *Journal of Vibration and Acoustics*, 139(1):011009, 2017.

[10] Hao Zhu, Weidong Zhu, Yumei Hu, et al. Periodic response of a timing belt drive system with an oval cogged pulley and optimal design of the pitch profile for vibration reduction. *Journal of Computational and Nonlinear Dynamics*, 13(1):011014, 2018.

[11] Lingyuan Kong and Robert G Parker. Steady mechanics of belt-pulley systems. *Journal of Applied Mechanics*, 72(1):25–34, 2005.

[12] Masanori Kagotani and Hiroyuki Ueda. Transmission error due to resonance in synchronous belt drive with eccentric pulley. *Journal of Mechanical Design*, 139(12):123301, 2017.